AN INVESTIGATION OF THE THRUST AND SPEED TRANSIENTS IN AN AXIAL FLOW TURBO-JET ENGINE

H. S. AINSWORTH
H. O. CUTLER
E. P. YATES

AN INVESTIGATION OF THE THRUST AND SPEED TRANSIENTS IN AN AXIAL FLOW TURBO-JET ENGINE

by

H. S. Ainsworth, Lt. U. S. Navy

H. O. Cutler, Lt. U. S. Navy

E. P. Yates, Lt. U. S. Navy

SUBMITTED IN PARTIAL FULFILLMENT OF THE REQUIREMENTS FOR THE DEGREE OF

MASTER OF SCIENCE

at the

MASSACHUSETTS INSTITUTE OF TECHNOLOGY

(1951)

ABSTRACT

An Investigation of the Thrust and Speed Transients in an Axial Flow Turbo-Jet Engine

by

Lt. H. S. Ainsworth, U. S. Navy

Lt. H. C. Cutler, U. S. Navy

Lt. E. F. Yates, U. S. Navy

Submitted for the partial fulfillment of the Degree of Master of Science in the Department of Aeronautical Engineering on 18 May 1951.

The study of thrust and speed transients are becoming necessary in the design of gas turbine control systems. This investigation was begun to attempt to correlate experimental transient data with that obtained by analytical means.

Thrust and speed transients for a step fuel function were obtained by the operation of an XJ-32 WE-4 turbo-jet engine. Two analytical methods of correlation are presented, the NACA method developed by Otto and Taylor and the method developed by Lt. Yates. The NACA method was satisfactory for small increasing fuel steps, and the Yates method was satisfactory for both large positive and negative fuel steps. Although both methods were initially devised for a step fuel function, it seems probable that the second method could be used with high accuracy for any known fuel function.

The investigation was conducted by the authors at the Gas Turbine Laboratory, Massachusetts Institute of Technology, Cambridge, Mass., from September 1950 to May 1951.

Cambridge, Massachusetts
18 May 1951

Professor Shatswell Ober, Chairman
Departmental Committee on Graduate Students
Department of Aeronautical Engineering
Massachusetts Institute of Technology
Cambridge, Massachusetts

Dear Sir:

In partial fulfillment of the requirements for the degree of Master of Science in Aeronautical Engineering, we are herewith submitting our thesis entitled, "An Investigation of the Thrust and Speed Transients in an Axial Flow Turbo-Jet Engine."

Respectfully,

TABLE OF CONTENTS

TABLE OF CONTENTS (cont'd.)

An Investigation of the Thrust and Speed Transients in an Axial Flow Turbo-Jet Engine

INTRODUCTION

The purpose of this investigation was to determine analytically and to correlate by experimental tests, the transient phenomena encountered in an axial flow turbo-jet.

Some previous work has been done in this field using a somewhat similar approach (Ref. 1). However, the engine considered utilized a centrifugal flow compressor, which produced a flat compressor characteristic curve. It was believed that the method might be extended to axial flow compressor types, if the turbine nozzles were choked throughout the range of transient operation and where the acceleration was not so great as to drive the compressor through the surge line.

It was believed that such an investigation might lead to a method of analytically expressing the transient behaviour of axial flow turbo-jets from the component characteristics. Thus speed control device design might parallel the design of a particular engine and thereby reduce the "cut and try" practice to a minimum.

Two methods of analytically obtaining the transient operation were used. The first method required no exact knowledge of the component part characteristics, but utilized estimated performance data available in Ref. 2.

The second method employed the use of the compressor characteristics obtained from Ref. 4 and 5, and the geometry of the turbine. Slightly different results were obtained.

The experimental data was obtained from operation of a Westinghouse XJ-32 WE-4 turbo-jet engine.

This investigation was conducted by Lt. E. F. Yates, Lt. H. C. Cutler, and Lt. H. S. Ainsworth, United States Navy, under the supervision of Professor E. S. Taylor. The experimental work was performed in the Gas Turbine Laboratory at the Massachusetts Institute of Technology, Cambridge, Massachusetts.

The general assistance, cooperation, and advice of the following are gratefully acknowledged:

Professor E. S. Taylor

Dr. Y. T. Li

Mr. Rudolph Light

Mr. Ferdinand Lustwerk

Mr. J. F. Hands

Mr. Dalton Baugh

Mr. Basile Mesnjankine

U. S. Naval Air Station, Squantum, Mass.

U. S. Naval Shipyard, Boston, Mass.

EQUIPMENT AND PROCEDURE

The experimental data was obtained by operation of a Westinghouse XJ-32 WE-4 turbo-jet engine. Necessary mountings, accessories, and equipment were installed to measure transient engine speed, transient thrust, and all of the static equilibrium variables necessary for cycle computations and verification of manufacturer's data. A complete description of this installation and instrumentation is contained in Appendices B and C.

Preliminary tests were made to determine the accuracy of the manufacturer's data and the validity of results of the testing equipment. After consistency was established between the published data and testing apparatus, only transient data were recorded and the assumption was made that the equilibrium operation data did not vary.

A Highland lightbeam recording galvanometer was used for recording all transient data.

The turbo-jet was operated for approximately ten minutes at equilibrium before any data were obtained in order to insure a continuous non-varying fuel supply. Control was then taken away from the usual governor fuel control and the rpm was adjusted at 22,000. All equilibrium data were then checked. A fuel step was then added to the normal fuel flow by means of a Hoke valve inserted in the system (Appendix B). When the engine had stabilized at the higher rpm (after the fuel step was manually added), equilibrium data were then again checked. The galvanometer was started and the step fuel solenoid closed. Equilibrium was again obtained, the galvanometer was stopped. This operation gave a negative fuel step. In like manner, the solenoid valve was opened and a positive fuel step obtained. At the same instant of solenoid operation,

an indicator light in the galvanometer recorded the time (t=0) of the fuel step addition.

Four steps both positive and negative were recorded; the steps were approximately:

1. 22,000 to 24,000 rpm
2. 22,000 to 26,000 rpm
3. 22,000 to 28,000 rpm
4. 22,000 to 30,000 rpm
5. 30,000 to 22,000 rpm
6. 28,000 to 22,000 rpm
7. 26,000 to 22,000 rpm
8. 24,000 to 22,000 rpm

ANALYSIS AND DEVELOPMENT OF THEORY

In a control system the rate at which the control parameter should be varied is dependent upon the rate at which the dependent variable responds to changes in the independent variable. The most simple and direct method of controlling the thrust of a turbo-jet with fixed exhaust nozzle is by controlling the fuel flow, which in turn controls the engine speed, establishing the mass flow and thereby setting the thrust.

During equilibrium operation, the engine is operating at states (1), (2), (3), (4), and (5). When the fuel function is added, these states change to (1'), (2'), (3'), (4'), and (5'), respectively. The movement from (2) to (2') is dictated by the engine characteristic matching curve (Fig. 2). The movement from (3) to (3') is dictated by the enthalpy addition from the fuel. States (4') and (5') are then determined by the engine geometry. The difference between the enthalpy drop between (1) and (2'), and (3') and (4') determines the accelerating torque, Q. The difference between (4) and (5), and (4') and (5') determines the increase in thrust per pound.

In these analyses, the fuel flow was made the independent variable and rpm the dependent variable for which the transient response was desired. Two methods were developed; the first followed the general method of Ref. 1, and the second was completely developed by Lt. E. P. Yates, U.S.N.

Method A (NACA)

In the turbo-jet engine, operating at equilibrium at a fixed rpm, an increase in fuel flow increases the fuel-air ratio, thereby increasing

the turbine inlet temperature which results in an increase in torque on the turbine shaft. If this torque is not absorbed by some external torque on the shaft, the unit will accelerate according to the following

$$\alpha = \frac{Q}{I} \tag{1}$$

The preceding equation can be written in differential form:

$$I \frac{dN}{dt} = Q \tag{2}$$

It follows that the differential equation can be solved if the parameter Q can be expressed as a function of the dependent variable N and the independent variable, fuel flow (Wf). Therefore it may be written:

$$Q = f(\omega_f, N)$$

$$Q - Q_o = \frac{\partial Q}{\partial \omega_f} \Delta\omega_f + \frac{\partial Q}{\partial N} \Delta N \tag{3}$$

If equilibrium has been established prior to imposing the fuel function, Q_o (the excess torque) is zero by definition and the equation may be written:

$$Q = \frac{\partial Q}{\partial \omega_f} \Delta\omega_f + \frac{\partial Q}{\partial N} \Delta N \tag{4}$$

Eliminating Q from equations (4) and (2) gives:

$$I\frac{dN}{dt} = \frac{dQ}{d\omega_f}\Delta\omega_f + \frac{dQ}{dN}\Delta N \qquad (5)$$

Noting that $dN/dt = d(N - N_o)/dt = d\Delta N/dt$, equation (5) can be written:

$$I\frac{d\Delta N}{dt} - \frac{dQ}{dN}\Delta N = \frac{dQ}{d\omega_f}\Delta\omega_f \qquad (6)$$

which is a linear differential equation in ΔN and t.

If $(dQ/d\omega_f)$ and (dQ/dN) are considered constant throughout the transient state, and we designate these constants as "a" and "b" respectively, the solution to the equation takes the form:

$$N = N_o - \frac{a}{b}\Delta\omega_f\left(1 - e^{\frac{bt}{I}}\right) \qquad (7)$$

For any given engine, the moment of inertia is either known or easily determined from its component parts. It remains, therefore, to determine the constants "a" and "b", and for any given function in fuel flow, the time response of the engine speed can be calculated.

The constants "a" and "b" could be determined by considering each dynamic state during the transient as a quasi-static state with an excess torque supplied by the turbine for acceleration. This excess torque could be obtained from the matched characteristic curves for the turbine and compressor or from experimental data obtained by absorbing the excess torque (produced by increasing fuel flow) by means of a dynamometer geared to the turbine shaft.

For this investigation, the turbine and compressor characteristics

for the Westinghouse XJ-32 WE-4 were not originally available, nor was it practical to install a dynamometer rig for measurement of the quasi-static excess torque.

Data were available, however, on values of thrust, fuel flow, and rpm for various tail cone positions. The hypothesis was made that a portion of the increase in thrust (obtained by varying the tail cone position and increasing the fuel flow to maintain the rpm constant) could have been absorbed as torque in the turbine shaft had the tail cone position been unchanged, and a larger pressure drop taken across the turbine rather than in the exhaust nozzle.

It can be shown that for static operation and exhaust nozzle expansion to ambient pressure, the static thrust is given by:

$$F = (w_a + w_f)\frac{V_e}{g} \tag{8}$$

Thermodynamics shows that the static enthalpy drop in a nozzle expanding from an infinite reservoir is:

$$\Delta h = V_e^2/2gJ \quad BTU/lb. \tag{9}$$

Solving (8) for Ve and substituting into (9):

$$\Delta h = \frac{1}{2gJ}\left[\frac{F g_o}{w_a + w_f}\right]^2 \tag{9a}$$

and the total enthalpy drop is:

$$\Delta H = \frac{1}{2gJ}\frac{F^2 g_o^2 (\omega_a + \omega_f)}{(\omega_a + \omega_f)^2} = \frac{1}{2gJ}\frac{F^2 g_o}{(\omega_a + \omega_f)} \qquad (9b)$$

and the corresponding total power is:

$$P = \frac{F^2 g_o}{2(\omega_a + \omega_f)} \text{ ft. lb./sec.} \qquad (10)$$

and also:

$$P = 2\pi Q N \text{ ft. lb. rad./min.} \qquad (11)$$

It was assumed that the ratio of the isentropic turbine work to the total enthalpy drop from (3') to ($5'_{ss}$) was the same under transient conditions as under equilibrium conditions (Fig. 4). The actual turbine accelerating torque was then corrected for turbine efficiencies (Fig. 3) and the ratio between the turbine and nozzle efficiencies.

P was then eliminated between (10) and (11) and the resulting equation for the effective torque produced by the thrust was:

$$Q = \frac{196 F^2 \psi \eta_T}{N(\omega_a + \omega_f)\eta_n} \qquad (12)$$

For various values of N and tail cone position, the values of Q were calculated assuming $\eta_n = .95$.

The tail cone position for these experimental tests was set at 1.9 inches out (corresponding to design position of operation at 200 mph).

Thus, by assuming this position as the static equilibrium position or position of zero accelerating torque, the difference between the torque calculated for this tail cone position and that calculated for other tail

cone positions at the same rpm is the torque available for accelerating at that rpm for various incremental steps in fuel flow. The values of accelerating torque vs. fuel flow rate were plotted in Fig. 5 with rpm as a parameter. The slopes of these curves provide the constant "a" for the differential equation for specific values of Wf.

By crossplotting this curve with Wf as a parameter in Fig. 6, the constant "b" was obtained as the slope of the constant Wf lines.

Applying standard corrections to the rpm, fuel flow, and torque terms, it can be shown that (7) can be written in a form that corrects the values obtained to standard conditions. In this form (7) becomes:

$$\frac{\Delta N}{\sqrt{\theta}} = \frac{N_f + N_o}{\sqrt{\theta}}\left(1 - e^{\frac{b\,\delta t}{\theta I}}\right) \qquad (7a)$$

For simplicity in analysis and experimentation, a step fuel function was chosen.

By simple calculations of the maximum permissible fuel-air ratio, it was determined from a temperature consideration that the safe maximum step fuel function allowable when operating at an initial rpm of 22,000 was that which would cause an increase of 8,000 rpm. Equation (7) was, therefore, plotted for various values of $(N - N_o)/(N_f - N_o)$ for steps of approximately 2,000, 4,000, 6,000, and 8,000 rpm. These plots appear on Figs. 7a, 8a, 9a, 10, 11a, 12a, 13, and 14.

Method B (Yates):

This method was devised when the compressor, combustor, and turbine characteristics were made available to the authors. The analysis was based upon the turbine velocity triangle (Fig. 15) and the engine characteristic matching curve (Fig. 2).

It was assumed that the turbine operated as an axial impulse turbine with nozzles choked at all rpm's and further that the flow through the turbine rotor was incompressible.

Thus from Fig. 15, under choking conditions:

$$\frac{C_1'}{C_1} = \sqrt{\frac{T_3'}{T_3}} \tag{13}$$

$$C_{1u} = 2u \tag{14}$$

$$C_{1u}' = C_{1u}\left(\frac{C_1'}{C_1}\right) \tag{15}$$

$$w_2' = w_2\left(\frac{C_1'}{C_1}\right) \qquad \text{(assuming incompressible flow)} \tag{16}$$

$$w_{2u}' = w_{2u}\left(\frac{C_1'}{C_1}\right) = u\left(\frac{C_1'}{C_1}\right) \tag{17}$$

$$C_{2u}' = w_{2u}' - u \tag{18}$$

substituting (15) and (17):

$$\Delta C_u' = C_{1u}' + C_{2u}' = C_{1u}\left(\frac{C_1'}{C_1}\right) + u\left(\frac{C_1'}{C_1}\right) - u \tag{19}$$

now dividing by u:

$$\frac{\Delta C_u'}{u} = \frac{C_{1u}}{u}\left(\frac{C_1'}{C_1}\right) - 1 + \left(\frac{C_1'}{C_1}\right) \tag{20}$$

substituting (14):

$$\frac{\Delta C_u'}{u} = 3\frac{C_1'}{C_1} - 1 \tag{21}$$

From Fig. (15):

$$\frac{\Delta C_u}{u} = 2 \tag{22}$$

Then:

$$\delta\left(\frac{\Delta C_u}{u}\right) = \frac{\Delta C_u'}{u} - \frac{\Delta C_u}{u} = 3\left(\frac{C_1'}{C_1} - 1\right) \tag{23}$$

Where: is difference between the equilibrium and transient value at any rpm.

Now:

$$\frac{C_1'}{C_1} = \sqrt{\frac{T_3'}{T_3}} \tag{13}$$

or

$$\delta\left(\frac{\Delta C_u}{u}\right) = 3\left[\sqrt{\frac{T_3'}{T_3}} - 1\right]$$

$$= 3\left[\sqrt{1 + \frac{\Delta T_3}{T_3}} - 1\right] \tag{24}$$

$$\sqrt{1+\frac{\Delta T_3}{T_3}} \cong 1+\frac{1}{2}\frac{\Delta T_3}{T_3} \tag{25}$$

$$\therefore \quad \delta\left(\frac{\Delta C_u}{u}\right) \cong 3\left[1+\frac{1}{2}\frac{\Delta T_3}{T_3}-1\right] = 1.5\,\frac{\Delta T_3}{T_3} \tag{26}$$

$$P = \omega_a\left(\frac{u}{g}\Delta C_u\right) = \frac{\omega_a u^2}{g}\left(\frac{\Delta C_u}{u}\right) \tag{27}$$

$$\delta P = \frac{\delta\omega_a}{g}\,u^2\left(\frac{\Delta C_u}{u}\right) + \frac{\omega_a}{g}u^2\,\delta\left(\frac{\Delta C_u}{u}\right) \tag{28}$$

$$P = 2\pi n \tilde{T} \tag{29}$$

$$\delta P = 2\pi n\,\delta\tilde{T} \tag{30}$$

Let $\delta\tilde{T} = Q$ = accelerating torque.

Then:

$$\frac{2\pi N Q}{60} = \frac{\delta \omega_a u^2}{g}\left(\frac{\Delta C_u}{u}\right) + \frac{\omega_a}{g} u^2 \delta\left(\frac{\Delta C_u}{u}\right) \tag{31}$$

Then Q, the accelerating torque, is:

$$Q = \frac{2\pi N}{60 g_o} r^2 \left[2\delta\omega_a + 1.5\,\omega_a \frac{\Delta T_3}{T_3}\right] \tag{32}$$

To find effective mean radius, consider the equilibrium point:

$$P_{Turbine} = \omega_a \frac{u}{g_o} \Delta C_u \tag{33}$$

and for axial impulse stage turbine:

$$P_t = \frac{2\omega_a u^2}{g_o} = \frac{2\omega_a}{g_o} r^2 \omega^2 \tag{34}$$

Therefore:

$$r^2 = \frac{P_t g_o}{2\omega_a \omega^2}$$

or

$$r_{mean} = 12\sqrt{\frac{J\Delta h_t g_o}{2\omega^2}} = 12\sqrt{\frac{J\Delta h_c g_o}{2\omega^2}} \tag{35}$$

Substituting the values of the variables in equation (35) for various equilibrium operating points resulted in an r_{mean} value of 3.25 inches. This value was assumed constant over range of transient operation.

Then by substituting this value of r_{mean} in (32) and simplifying:

$$Q = .239\left(\frac{N}{1000}\right)\left[2\delta\omega_a + 27.8\frac{\Delta\omega_f'}{T_3}\right] \qquad (36)$$

where: $\Delta\omega_f'$ = Fuel flow in excess of the fuel flow for equilibrium operation at any rpm.

For simplicity of analysis and experimentation, a step fuel function was assumed, introduced at zero time. The value of $\Delta\omega_f'$ was determined for various rpm's by subtracting the furl flow at equilibrium operation from the actual fuel flow introduced. The equilibrium values were obtained from Fig. 16.

The values of T_3 for given rpm were obtained from the following equation:

$$\Delta T_3 = 18.55\frac{\Delta\omega_f'}{\omega_a} \qquad (37)$$

where: $\Delta\omega_f'$ = lbs/hr.

The values of T_3 for given rpm were also taken from Fig. 2. From the equation:

$$Q = I\alpha = I\frac{dN}{dt} \qquad (38)$$

where: I = .226 lb in. sec^2 (Ref. 2)

and substituting equation (36) into (38)

$$\frac{dN}{dt} = 121\left(\frac{N}{1000}\right)\left[2\delta\omega_a + 27.8\frac{\Delta\omega_f'}{T_3}\right] \qquad (39)$$

then:

$$\frac{dt}{dN} = \frac{1}{\frac{dN}{dt}} = \phi_N$$

The values of dt/dN were plotted versus N, an example of which is shown in Fig. 17.

Then

$$\int_{t_0}^{\tau} dt = \int_{N_0}^{N} \phi_N \, dN \tag{40}$$

The integration indicated was performed graphically.

Various step fuel functions were assumed and the above calculations performed. The resulting acceleration curves were plotted in Figs. 7b, 8b, 9b, and 12b.

Thrust Transient Analysis

Basic analysis shows that for static operation, the thrust can be determined by:

$$F = \omega_a V_e/g \qquad \text{(neglecting the small value } \omega_f\text{)} \tag{8}$$

and during transient operation, the thrust, F', will be:

$$F' = \omega_a' V_e'/g \tag{41}$$

Thermodynamics gives the following:

$$\frac{V_e'^2}{2gJ} = h_4' - h_5' = W_N' \tag{42}$$

$$h_3' - h_{5'ss} \cong \frac{W_c'}{\eta_t} + \frac{W_\varphi'}{\eta_c'} + \frac{W_N'}{\eta_c'} \tag{43}$$

Solving for W_N':

$$\frac{W_N'}{\eta_n'} = (h_3' - h_{5s}') - \frac{W_c'}{\eta_t'} - \frac{W_Q'}{\eta_t'} \tag{44}$$

$$W_c' = h_2' - h_1' = \frac{c_p T_1'}{\eta_c}\left[\left(\frac{P_2'}{P_1'}\right)^{\frac{k-1}{k}} - 1\right] \tag{45}$$

$$W_Q' = W_T' - W_T = \frac{2\pi N Q}{\omega_a' J 60} \tag{46}$$

$$h_3' - h_{5s}' = c_p T_3\left[1 - \left(\frac{P_1'}{P_2'}\right)^{\frac{k-1}{k}}\right] \tag{47}$$

After solving for Ve', the above gives:

$$F = \frac{\omega_a'}{g}\sqrt{2gJW_N'} \tag{48}$$

Since the values of W_a' and W_N' were obtained as a function of rpm, thrust can be plotted as a function of time.

RESULTS AND DISCUSSION

Seventy-six runs were made with the described apparatus, but because of mechanical recording difficulties, data for only forty-four were obtained. Since it was very difficult to obtain the exact desired rpm step by means of the auxiliary fuel system solenoid step valve, a number of the runs were either slightly below or above the desired rpm step. The runs of the same rpm step were reproducible as far as both thrust and speed were concerned. The data plotted on semi-log paper as nearly exact straight lines, indicating an exponential relationship with time.

Eight of the best runs, that is, those that were the closest to the desired rpm steps, were replotted from the oscillograph recording paper onto Figs. 7a through 14. The analytical transients of method A and B were plotted on the "a" and "b" curves of Figs. 7a to 14 respectively.

Method A:

Method A was essentially the same as that used in other investigations and explained in detail in Ref. 1. A slight variation in the method of obtaining the parameter $(\partial Q/\partial N)$ was necessitated because complete component characteristics were not available at the time the analytical computations were made. The three assumptions made: (a) that the ratio between the enthalpy drop across the nozzle and the total enthalpy drop from the turbine inlet to nozzle outlet was constant at any given rpm regardless of fuel flow, (b) that the nozzle efficiency remained constant at 95%, and (c) that the coefficients of equation (3) were constant, were substantiated by the results of Method B within the accuracy of other computations.

Previous investigations, reported in Ref. 1, have produced similar results with the use of this method, in that good correlation between analytical and experimental results were obtained for small positive step fuel functions, with poor results for negative steps and large positive steps. The authors of this report, however, do not agree completely with the authors of Ref. 1 in their reasons for the poor correlation. The assumption that the rotor losses are appreciably increased due to the small reduction in angle of incidence accompanying a reduction in the turbine inlet temperature is not believed substantiated by present day tests. However, consideration of equation (32) and the characteristic curve from which the values for solution were obtained readily indicate the reason for deviation from theoretical calculations. It can be noted that the accelerating or decelerating torque is a function of $N, \delta\omega_a, \omega_a$, and $\Delta T_3/T_3$. Having fixed $\Delta T_3/T_3$, the parameters N, $\delta\omega_a$ (a negative value), and ω_a, all vary in such a manner as to produce higher decelerating torques at high rpm than accelerating torques at low rpm. The magnitude of these effects are greatly affected by the slopes of the constant rpm lines on the compressor map.

The explanation given in Ref. 1 for the slower response rate and poor correlation for high step fuel functions places the cause on the reduced combustion efficiency as approach to acceleration blowout is made. Combustion chamber experiments do not substantiate such reasoning to the extent necessary to cause a noticeable change in the time response. Again referring to equation (32) and the engine characteristic matching curve, it can be shown that the $\delta\omega_a$ term is a dominating factor and increases as the magnitude and rate of the fuel function is increased, thereby reducing the transient response below that calcu-

lated by Method A.

Method B:

The results of Method B are considered to be excellent in that they demonstrate analytically and quantitatively the various trends observed in the data obtained. The apparently poor correlation at low step functions in fuel flow are not an indication of a limitation on the use of the method, but indicate the need of more accurate recording methods, of expanded plots of the engine characteristic matching curve, and the use of highly accurate calculations in order to eliminate the large percentage errors obtained in taking differences between large numbers. The graphical method of integration produces larger errors in the calculations of the small steps since fewer points on the dt/dN curve were used.

Since the exact fuel function obtained was not measured and since it is unlikely that an exact step was obtained, it is probable that the variation from the step is more important for the small steps than for the large steps. Consideration of this effect on the parameter $\delta\omega_a$ will show that less than an exact step in turbine inlet temperature may increase the initial acceleration of the engine over that obtained by an exact step.

Assuming a path on the engine characteristic curve, a fuel function can be calculated which would give nearly exact correlation between thrust and rpm. It is a matter of conjecture whether this function would be the exact function obtained in practice or a summation of this function and all the errors made in the recording and calculation. A highly accurate and tedious analysis would be required before further comment could be made.

CONCLUSIONS

It is concluded that:

a) The assumption of constant coefficients in the engine control differential equation used in Method A seems reasonable for small fuel steps but not as accurate for large fuel steps.

b) The method B explained herein appears to give good results for any fuel function and is restricted only by the accuracy of component part characteristics and accuracy of calculation.

c) Given any fuel flow as a function of time, the transient behaviour of the engine can be accurately calculated by Method B.

RECOMMENDATIONS

The mounting and installation of the turbo-jet was adequate and should suffice for many other investigations. The governor control and manual control give completely flexible operation. The direct reading instruments required to operate the turbo-jet were dependable and accurate. The thrust and rpm transient measurements worked well for this study. The thrust measurement system picked up and recorded a sine-wave oscillation. This oscillation could have been the natural frequencies of the retaining system or it could have been some regular variation of thrust during the transient run. It is recommended that the retaining system be altered to eliminate possible interference with the thrust transient.

For any more detailed investigations further instrumentation is desirable. Since this investigation was in the field of transients, most recommendations deal with continuous, rapid, recording. For instance, it would be advantageous if air mass flow and fuel flow could be recorded continuously. An orifice coupled with a strain gage pressure measuring device as described in Ref. 6 would undoubtedly be adequate. A recording rotameter would also suffice for recording fuel flow provided the lag were not appreciable. Continuous recording of pressures and temperatures would also be desirable.

The light beam recording galvanometer used for this investigation was difficult to use since the paper strip had to be developed each time to check results. Further, the paper driving mechanism slipped several times and many runs were lost whereas the malfunction would have been immediately evident on another type galvanometer. Also, a wider strip than the four inches used is recommended for increased accuracy.

The turbo-jet used for this study was typical of most axial flow engines and should therefore be adequate for enumerable investigations.

In control and transient phenomena, the step fuel input is the most simple possible function and is almost never attained or used in practice. The introduction of fuel inputs typical of control mechanisms and the correlation of analytical and actual data would be an extremely practical investigation.

In the field of control, the tendency appears to be toward electronic control mechanisms. A collaboration between electronic and turbine thesis students should offer interesting design possibilities.

Studies could be conducted on the effect of the introduction of water and other liquids into the compressor inlet. The effect of fuel additives such as powdered metal could also be investigated.

Inasmuch as the XJ-32 WE-4 (9.5") is essentially a one-half scale model of the J-30-WE (19.0") turbo-jet and since considerable data is available on the J-30-WE-4 engine, similarity studies similar to those done on internal combustion engines could be conducted.

It is believed that further thought and study would lead to an easy method of determining the solution to the equations of Method B and the results presented in a readily usable manner. The results of such a study should be of great value to control designers and engineers.

REFERENCES

1. Otto, Edward W., and Taylor, Burt L.: Dynamics of a Turbojet Engine Considered as a Quasi-Static System. NACA TN 2091, 1950.

2. Handbook of Service Instructions with Parts Catalog for Turbo-jet Engines Model XJ32-WE-4.

3. Westinghouse Electric Corp.: Turbojet Aviation Engine Log Book, Serial WE001040, 1947.

4. Negulici, Charles, and Billy, W. S.: Performance of Westinghouse 9.5A Six-Stage Axial Flow Compressor. NACA MR No. E5L07, 1945.

5. Bogart, Donald; Simulated Altitude Performance of Combustors for the 9.5 Jet Engine, II - 9.5 Combustor. NACA RM No. E7B21.

6. Li, Dr. Y. T., and Draper, Dr. C. S.: A New Pressure Indicator of the Strain Guage Type. Journal of the Aeronautical Sciences, Oct. 1949.

7. Fischer and Porter Co.: Technical Report, Technical Bulletin No. A-90-4.

Sample Calculations

Method A. (NACA)

Known or Assumed:

1) rpm = 22,000

2) Exhaust Nozzle Position (Ref. 2)
   a) 1.9 inches out
   b) 2.3 inches out

3) Fuel Flow (Ref 2)
   a) W_{f_a} = .0572 lb/sec
   b) W_{f_b} = .0619 lb/sec

4) Thrust (Ref 2)
   a) F_a = 88 lbs.
   b) F_b = 95 lbs.

5) Mass Flow (Ref 2)
   a) $W_a + W_f$ = 3.92
   b) $W_a + W_f$ = 3.93

6) Ratio between isentropic turbine work to total enthalpy drop. (Fig 4., calculated from data contained in Ref 2.)
   a) Ψ = 0.83
   b) Ψ = 0.83

7) Turbine efficiency (Fig. 3., calculated from data contained in Ref. 2)
   a) η_t = 0.62
   b) η_t = 0.62

8) Nozzle efficiency (assumed)
   a) η_n = 0.95
   b) η_n = 0.95

Calculation

Using equation (12):

$$Q_a = \frac{146\,(88)^2(.83)\,(.62)}{22{,}000\,(3.92)(.95)} = 7.12$$

$$Q_b = \frac{146\,(95)^2(.83)(.62)}{22000.\,(3.93)(.95)} = 8.25$$

The accelerating torque is then obtained by subtracting the torques calculated for the two tailcone positions:

$$Q = Q_b - Q_a = 8.25 - 7.12 = 1.13 \text{ ft lb.}$$

This value of accelerating torque would be obtained for a step fuel function corresponding to:

$$\omega_{f_a} = .0572 \text{ lb/sec}$$

to

$$\omega_{f_b} = .0619 \text{ lb/sec}$$

Method B (Yates)

Known or assumed:

1.) rpm = 22,000

2.) Axial flow, fixed exhaust area, turbo-jet

3) Engine matching curve (Fig 2)

4) Magnitude of step fuel function

$$\Delta\omega_f = 74 \text{ lb/hr}$$

5) $c_p = .286$ from T_3 to T_5

Calculation

1.) Enter Fig. 2., and at 22,000 rpm find ω_a and T_3:

$\omega_a = 3.94$ lb/sec } Steady state

$T_3 = 1600\ ^\circ R$ }

2) Compute ΔT_3 from magnitude of step fuel function and ω_a.

$$\Delta T_3 = 18.5 \frac{\Delta w_f}{\omega_a} = 18.5 \times \frac{74}{3.94} = 347^\circ R$$

3) Entering Fig 2 again at 22,000 rpm and $T_3' = T_3 + \Delta T_3 = 1950^\circ R$, find ω_a'

$$\omega_a' = 3.72 \ lb/sec$$

4) $\delta \omega_a = \omega_a' - \omega_a = 3.72 - 3.94 = -.22 \ lb/sec$

5) Using equation (36)

$$Q = .239 \left(\frac{22000}{1000}\right)\left[2(-.22) + 27.8 \frac{74}{1600}\right] = 4.42 \text{ ft lb.}$$

This value of Q is the accelerating torque obtained by a step function of 74 lb/hr at an engine speed of 22,000 rpm.

6) Using Eq. (39)

$$\frac{dN}{dt} = 121\left(\frac{22,000}{1000}\right)\left[2(-.22) + 27.8 \frac{74}{1600}\right] = 2230 \ \frac{rpm}{sec}$$

7) $\frac{dt}{dN} = \frac{1}{2230} = .449 \times 10^{-3} \frac{sec}{rpm}$

8) $t = \int_{N_0}^{N} \frac{dt}{dN} dN$ (done graphically, Fig 17)

9) Enter Fig 2. at 22000 rpm and $T_3 = 1947^\circ R$ and find $\frac{P_2'}{P_1} = 1.74$

10) $\Delta h_{\text{total isentropic}} = C_p T_3' \left[1 - \left(\frac{1}{\frac{P_2'}{P_1}}\right)^{\frac{K-1}{K}}\right]$

$$= .286\,(1947)\left[1 - \frac{1}{1.74}^{\frac{1.93-1}{1.93}}\right] = 70.5 \frac{BTU}{lb}$$

11) $W_c = \frac{.24\,(520)}{73}\left[(1.74)^{\frac{1.4-1}{1.4}} - 1\right] = 25.1 \ \frac{BTU}{lb}$

12) $W_Q = \frac{2\pi (4.42)(22.000)}{J\ 60(3.71)} = 3.54 \ \frac{BTU}{lb}$

13) $W_N = .95\left(70.5 - \frac{25.1 + 3.54}{.62}\right) = 23 \ \frac{BTU}{lb}$

14) $\%\Delta F = \frac{\omega_a' \sqrt{W_N} - \omega_{a_\theta} \sqrt{W_{N_0}}}{\omega_{a_f} \sqrt{W_{N_f}} - \omega_{a_0} \sqrt{W_{N_0}}}$

$= \frac{18 - 14.8}{27.5 - 14.8} = 25.2\ \%$

This value is the ratio between the change in thrust from equilibrium to transient at 22,000 rpm and the total change from equilibrium to equilibrium corresponding to a step fuel function of 74 lb/hr.

APPENDIX A

Symbols

The following symbols have been used throughout this report:

Ai	compressor inlet area - 33 $in.^2$
a	$\frac{\partial Q}{\partial \omega_f}$
b	$\frac{\partial Q}{\partial N}$
CIP	compressor inlet pressure - $lb/in.^2$
COP	compressor outlet pressure - $lb/in.^2$
CIT	compressor inlet temperature - ^oR
COT	compressor outlet temperature - ^oR
DPDT	double pole double throw switch
DPST	double throw single throw switch
f	final state
g	gravitational constant - 32.2 ft/sec^2
J	Joules' constant - 778 ft lbs/ btu
k	ratio of specific heats (1.4 for compressor)(1.33 in turbine)
I	mass moment of inertia of rotating parts (.226 in. lb sec^2)
N	engine speed rpm
o	subscript refers to initial state
P	power
p	pressure - $lb/in.^2$
p_a	ambient pressure - $lb/in.^2$
Q	accelerating torque - lb-ft
r_m	effective mean radius

s	subscript refers to isentropic path
SPDT	single pole double throw switch
SPST	single pole single throw switch
TIP	turbine inlet pressure - lb/in.^{2}
TOP	turbine outlet pressure - lb/in.^{2}
TIT	turbine inlet temperature - ^oR
TOT	turbine outlet temperature - ^oR
t	time - seconds
Ve	effective exhaust velocity - ft/sec
w_a	air flow - lb/sec
w_f	fuel flow - in units indicated
W_c	compressor work - btu/lb
W_n	nozzle work - btu/lb
W_Q	acceleration work - btu/lb
W_t	turbine work - btu/lb
α	angular acceleration - radians/sec
δ	difference between equilibrium and transient value at any rpm (also indicates p/14.7)
ϕ_N	dt/dN at any rpm
τ	torque
θ	T/518.7
ψ	$\frac{\text{equilibrium isentropic turbine work}}{h_3 - h_{5_{ss}}} = \frac{\text{transient isentropic turbine work}}{h_3' - h_{5_{ss}}'}$
η_T	turbine efficiency
η_c	compressor efficiency
η_N	nozzle efficiency
ρ_a	ambient density - lb/ft^3
ω	angular velocity - rad/sec
'	superscript refers to transient path

APPENDIX B

Installation Description

Engine (complete specifications contained in Ref. 2)

The jet engine used for this investigation was an XJ-32 WE-4 (9.5 inch) Westinghouse gas turbine jet. It was an axial flow type with a six-stage compressor giving a nominal pressure ratio of three-to-one. The combustion chamber was an annular type and combustion once started was self-sustaining. The turbine was a single-stage turbine directly coupled to the compressor rotor. The accessory group was driven by a splined shaft from the front end of the compressor rotor shaft at a speed reduction of 1:10. The accessories consisted of a lubricating oil pump, fuel pump, tachometer generator, and a flyweight fuel governor.

The military rating of the engine was 260 lbs. thrust at 34,000 rpm with a fuel flow of 420 lbs/hr and a mass flow of 6.5 lbs/sec. The approximate dry weight of the engine was 150 lbs.

Mounting and Cradle (Figs. 18 and 19)

The turbine was mounted as specified in Ref. 2. The main thrust absorbing mounting was that provided in the packing case which supports the engine at the compressor outlet section. A rear mounting which did not take thrust was connected to the rear mounting lug for longitudinal stability. The mounting was rigidly fastened to an angle iron frame suspended from the overhead by means of steel cables. The purpose of the cable suspension was to provide a near frictionless mounting for transient thrust measurement. In order to eliminate the possibility of the turbine

weight introducing components which would affect the thrust measurements, the cables were hung vertically with respect to the forward and aft motion of the turbine. To prevent lateral oscillations, diagonal cables were rigged between the two front cables and also between the two rear cables. Forward motion of the turbine and mount was restricted by the strain gauge.thrust measuring device. An initial tension was placed upon the strain guage.

Fuel System (Fig. 20)

The fuel system as installed on the turbine consisted of a positive displacement fuel pump, a pressure relief valve set at 275 psig, a fuel solenoid shutoff valve, a fuel regulating flyweight governor, and the nozzle manifold ring.

Exterior to the turbine the fuel system consisted of a 1,000 gallon gasoline tank, an electrically driven positive displacement pump, a pressure relief valve, and a bank of rotameters for measuring fuel flow.

In addition, an auxiliary fuel metering system was installed for two reasons: first, to get a more flexible control than that provided by the governor, and second, to obtain a step fuel function as required for the type analysis undertaken. The auxiliary fuel metering system ran from the pressure relief discharge side to the fuel nozzle manifold. The auxiliary system consisted of two parallel systems: the primary metering side and the step function metering side. The primary metering side contained a needle type metering valve which replaced the fuel governoring system. The step function metering side contained a solenoid valve which working in conjunction with the primary metering side of the

auxiliary system provided a step fuel function.

The test operating procedure was as follows:

1) with the auxiliary system cut off, the turbine was started on the main fuel system (governor controlled system),

2) with the step function side of the auxiliary fuel system cut off the primary side of the auxiliary system gradually took control of the fuel flow until the main system was cut out by shutting the main fuel solenoid valve,

3) by opening the solenoid on the step function side of the auxiliary system the step fuel function was introduced, the magnitude of the step having been determined by the setting of the fuel step metering valve,

4) when step (3) was commenced with the step function side of the auxiliary system open, a negative fuel step function was obtained by closing the step function solenoid valve.

Electrical System (Figs. 21 and 22)

The electrical system was energized by means of a 24 volt aircraft battery tapped at the middle for a 12 volt servo motor supply. Two heavy wire conductors were led from the plus and minus battery terminals to the center of a DPDT switch. A voltmeter was connected to one side of this switch for checking battery voltage. The other side was led to two bus bars (+ red and - black).

The 12 volt battery positive tap was led directly to the center of a SPST servo motor switch. Three momentary switches controlled the servo motor as it positioned the governor.

The air and fuel valve solenoids were controlled by means of SPDT momentary switches. Two ignition coils were energized by means of a SPST momentary switch.

In addition to the usual electrical control system, a SPDT momentary switch was connected to a fuel solenoid valve on the auxiliary step fuel system. An SPDT switch controlled an electrical signal to the recording galvanometer to indicate the instant of operating the step fuel solenoid.

The bearing thermocouples were led directly to their respective indicators. However, the TOT and CCT were led to a six-channel rotary selector switch which was so arranged that the TOT could be read directly on an indicator connected to the TOT banana plugs on the panel or read on a potentiometer connected to the "potentiometer" receptacles. By means of a SPDT switch ("TOT") the TOT could be switched to either the potentiometer or the indicator (in this case a calibrated millivolt meter). The CCT could also be measured directly on this same potentiometer by merely switching the rotary selector switch from 1 to 2.

The electrical system of the control panel was connected to the turbine test stand terminals by means of a 30 conductor "T and T" shielded cable with the conductor markings as indicated in Fig. 21.

Charging System (Fig. 21)

The battery charging system was energized by a 115 volt D.C. supply led to the control panel to a large fused DPST switch. The voltage to the battery terminals was controlled by a 60Ω variable resistor in series with the power supply and battery. For charging, it was necessary to close the DPST knife switch. However, to prevent any injury to the servo motor and any delicate instruments, it was deemed advisable to disconnect

the 12 volt battery tap, open all power switches and throw the main battery switch to the voltmeter position before charging

Ducting and Bell-Mouth Inlet (Figs. 18 and 19)

Ducting was installed to discharge the turbine exhaust to the muffler of the test cell. The ducting was 13 inches in diameter, 16 gauge, galvanized sheet metal pipe. In order to maintain easy access to the test cell it was necessary to make one section of the ducting readily removable.

In addition, to prevent separation at the entrance to the compressor, which would reduce the mass flow and thereby cause dangerous overheating, it was necessary to install a bell-mouth intake on the compressor section.

Fire Extinguishing System (Figs. 18 and 22)

For emergency use and to insure complete extinguishing of combustion, a carbon dioxide system was installed. The system consisted of a CO_2 bottle and valve, a hose connection, and a pipe nozzle pointing into the compressor inlet. The bottle was inverted so that liquid CO_2 was forced through the lines and snow was produced at the nozzle.

APPENDIX C

Instrumentation

Thrust Measurement (Fig. 23)

Conventional methods of thrust measurements, involving the use of springs hydraulic piston and dash pot, or similar devices, were not suitable for the measurement of varying thrust loads due to their inherent time constants, hunting, and awkward recording instruments.

For this investigation, a modification of the sensitive element of a high performance pressure indicator of the strain gauge type was used. This gauge was designed by Dr. Y. T. Li and Dr. C. S. Draper and reported in Ref. 6.

The advantages of this type gauge over the ordinary strain gauge were: (a) higher sensitivity, (b) less sensitivity to ordinary variations in temperature, (c) higher factor of safety, and (d) more linear characteristics.

The sensitive element consisted of a hollow, steel tube wound circumferentially and longitudinally with high resistance cupron wire, 234 ohms per foot, diameter .0011 inches. Each end of the tube was tapped to receive a 3/8 inch bolt. The bolts were drilled and silver soldered onto 1/8 inch cable which was connected between the engine mounting frame and a stationary stand so as to absorb the entire thrust of the engine. When a tension load was applied to the tube the longitudinal winding increased in electrical resistance; at the same time the circumferentially wound coil experienced a reduction in resistance due to compressive strain. These two windings formed two arms of a balanced

bridge and the additive effect of the changes in resistance in each produced an output signal proportional to the applied thrust.

Because the windings were intimately bound to the strain generating tube, they closely followed temperature changes in the tube and received similar resistance changes due to a change in temperature of the tube and wire. As a result no potential change occurred at the output terminal because of temperature effect. In addition to this, the stress/strain ratio held a constant value, despite temperature changes, because of the compensatory effect between the change in modulus of elasticity and the change in Poisson's ratio of the strain tube. An asbestos plate shielded the strain gauge from the high exhaust temperatures.

The signal output of the gauge was amplified by an SR-4 strain gauge meter and recorded on photographic tape by the trace from a light beam galvanometer.

Engine Speed Measurement (Fig. 24)

The tachometer generator supplied with the engine was a three-phase generator, and its signal output was not found readily usable with the type of recorder available for this investigation due to non-constant voltage-speed ratio. This speed indicator system was used, however, for operational purposes and calibration of the speed recording system.

The latter system consisted of a direct current generator, with linear characteristics. the shaft of which was splined to the accessory section drive shaft.

The signal output from this generator was led through the galvanometer control circuit to the input terminal of the light beam recording galvanometer.

Galvanometer Sensivity Control System (Fig. 24)

A Highland light beam recording galvanometer was used in this investigation for recording transient data. It produced records on light sensitive paper, four inches wide, which moved perpendicularly to the direction of travel of the light beam at the rate of three inches per second.

The maximum throw of the light beam source without overloading the galvanometer was the equivalent of 32 inches or eight times the width of the recording band. In this investigation it was necessary to record small changes in rpm as low as from 22,000 to 24,000. If the full width of the paper were used to record this change, a sensitivity factor of two inches per 1,000 rpm would have been required. However, this caused the full throw of the light beam source to correspond to 48 inches, which exceeded the limits of the instruments. To eliminate this restriction on sensivity, a 45 volt battery and a potentiometer were introduced into the circuit to oppose the voltage of the tachometer and thereby move the null point to an rpm corresponding to the tachometer voltage of 45 volts. The potentiometer was used to reduce the battery voltage opposing the tachometer so that a null could be maintained as required.

The galvanometer sensivity control contained two voltage dividers which controlled the ratio of galvanometer input voltage to voltage output of the sensing elements: the strain gauge and tachometer generator. By varying this voltage ratio, the sensivity of the galvanometer could be varied at will, not to exceed the above-mentioned limits.

Suitable capacitors were installed across the tachometer and thrust gauge input to damp out the undesirable high frequency disturbances in the system.

Pressure Measurements

Though no use was made of the pressure data except as a check on the engine operation and as a crosscheck to insure consistency between the manufacturer's data (used for analytical calculation) and the actual results obtained, total pressure tubes and gauges were installed for measurement of total head at the compressor outlet, turbine inlet, and turbine outlet. The gauges were mounted on the control panel outside the test cell.

The dynamic head at the compressor inlet was obtained by pressure differential between test cell ambient and compressor inlet static pressures measured by "U" tube with fluid specific gravity of .846. The "U" tube was mounted on the control board outside the test cell.

The values of pressure differential were converted to mass flow by the following formula:

$$w_a = .9\, A_i \left[P_a \left(\frac{P_c}{P_a} \right)^{1/k} \right] \sqrt{2 g_o \left(\frac{k}{k-1} \right) \frac{P_a}{\rho_a} \left[1 - \left(\frac{P_c}{P_a} \right)^{\frac{k-1}{k}} \right]}$$

Fuel Flow

Fuel flow was measured by means of Fischer-Porter STABILVIS rotameters. In spite of claims of 1/2 per cent accuracy (Ref. 7), the rotameters were calibrated throughout their entire range by using gasoline and a balance scale. The method of calibration was standard: a stop

watch was started when the weight of the fuel caused the balance to tip, a delta weight was placed on the balance, and the watch was stopped when the balance tipped a second time. While the error in the upper and lower ranges was determined to exceed 1/2 per cent, the overall accuracy was sufficient for the investigation.

Three rotameters were used to cover the entire range. The two low scale rotameters were calibrated directly in pounds per hour and the high scale rotameter was calibrated in gallons per hour. All instruments were calibrated for aviation grade gasoline with a specific gravity of .69 to .74.

Temperature Measurement

Temperature was measured by means of five thermocouples:

1. No. 1 Main Bearing
2. No. 2 Main Bearing
3. No. 3 Main Bearing
4. Compressor Outlet Temperature
5. Turbine Outlet Temperature.

The bearing thermocouples were connected directly to three aircraft cylinder head temperature gauges. These gauges and thermocouples were calibrated at 100°C. It is to be noted that at room temperature these gauges did not read alike since the lead-in wires were not those specified by the manufacturer. However, at the operating temperatures, the readings were correct.

The CCT and TCT thermocouples were connected individually to two junctions immersed in a thermos bottle filled with ice water. These

leads were connected directly to a millivoltmeter and also to two female banana plug outlets through a six-channel rotary switch. The CCT was also led to this rotary switch. By connecting a millivolt reading potentiometer to the banana plug outlets, an accurate CCT or TCT could be measured on the potentiometer scale depending upon the channel selector position. In addition, a direct continuous TCT reading was indicated on the millivoltmeter.

APPENDIX D

Turbo-Jet Operation

The operation of the XJ-32 Westinghouse turbo-jet as installed in the Gas Turbine Laboratory at the Massachusetts Institute of Technology is herewith listed step by step for the different modes of operation. It is important that these procedures be followed exactly in order to prevent excessive temperatures and consequent turbine blade failure.

(1) Starting Check-Off List (Pre-Start)

1. Open lubricating valve.
2. Check battery voltage by moving switch to "volts".
3. Close main fuel solenoid valve.
4. Close step fuel valves.
5. Close air solenoid valve.
6. Open main air valve under test cell.
7. Check readiness of hand fire extinguishers and asbestos gloves.
8. Open CO_2 supply momentarily to check supply.
9. Close manual fuel valve.
10. Check 12 volt supply for availability.
11. Fill thermos bottle with ice and check TCT gauge for room temperature reading.

(2) Starting

1. Battery "on".
2. Servo 12 volts "on".

3. Depress "C" switch and visually check movement of control arm to center position.
4. Switch fuel booster pump "on".
5. Open manual fuel valve.
6. Check fuel booster pressure (12 psig).
7. Switch air solenoid valve to "open". Watch rpm for indication.
8. Open main fuel solenoid valve at 4,000 rpm.
9. Ignition switch "on" immediately.
10. Acceleration should be immediate and stabilize at 18,000 rpm.
11. Close air solenoid valve.
12. Check TCT gauge (about 1100°F $\pm$ 100°F). If temperature is too high, immediately close fuel solenoid valve and investigate possible causes.

(3) Speed Control Operation (Governor)

1. Operation of the "C" switch will cause the turbine to accelerate or decelerate to about 18,000 rpm.
2. Operation of the "M" switch will cause acceleration to maximum rpm.
3. Operation of "idle" switch will cause deceleration to 12,000 rpm.

(4) Speed Control Transfer Procedure

1. Accelerate to about 20,000 rpm by means of "Max" switch. Wait for stabilization.

2. Open main valve on auxiliary metering system panel.
3. Open primary metering valve gradually, maintaining 20,000 rpm by depressing the idle switch.
4. When the control arm reaches the full idle position, cut out the governor system by closing the main fuel solenoid valve. (This should cause a drop in rpm which can be picked up with the metering valve as before.)
5. With the main fuel solenoid valve closed, the governor is cut out and the control is solely the primary metering valve. Therefore, the TOT and rpm must be watched very carefully to avoid unsafe conditions.
6. Adjust primary metering valve very slowly to obtain desired rpm.

(5) Transient Operation

1. After taking over control with the auxiliary speed control system, open the step fuel solenoid valve.
2. Slowly open the step fuel metering valve until the rpm is that desired for the final equilibrium speed.
3. Close the step fuel solenoid valve (this will be the negative fuel step).
4. When equilibrium is reached, open the step fuel function solenoid valve (this is the positive fuel step).

To obtain the exact rpm change desired, it may be necessary to make several trials and errors before the precise step has been obtained.

(6) Stopping (from governor control)

1. Decrease to idle.
2. Close main fuel solenoid valve.
3. Check for fire in exhaust nozzle when rpm 0. If there is a fire, open CO_2 valve until fire is extinguished (approximately 3 to 5 seconds).

(7) Stopping (from manual control

1. Close the primary valve slowly to approximately 15,000 rpm.
2. Close manual valve of the auxiliary system and close the primary metering valve.
3. When rpm 0, check for fire as under governor control.

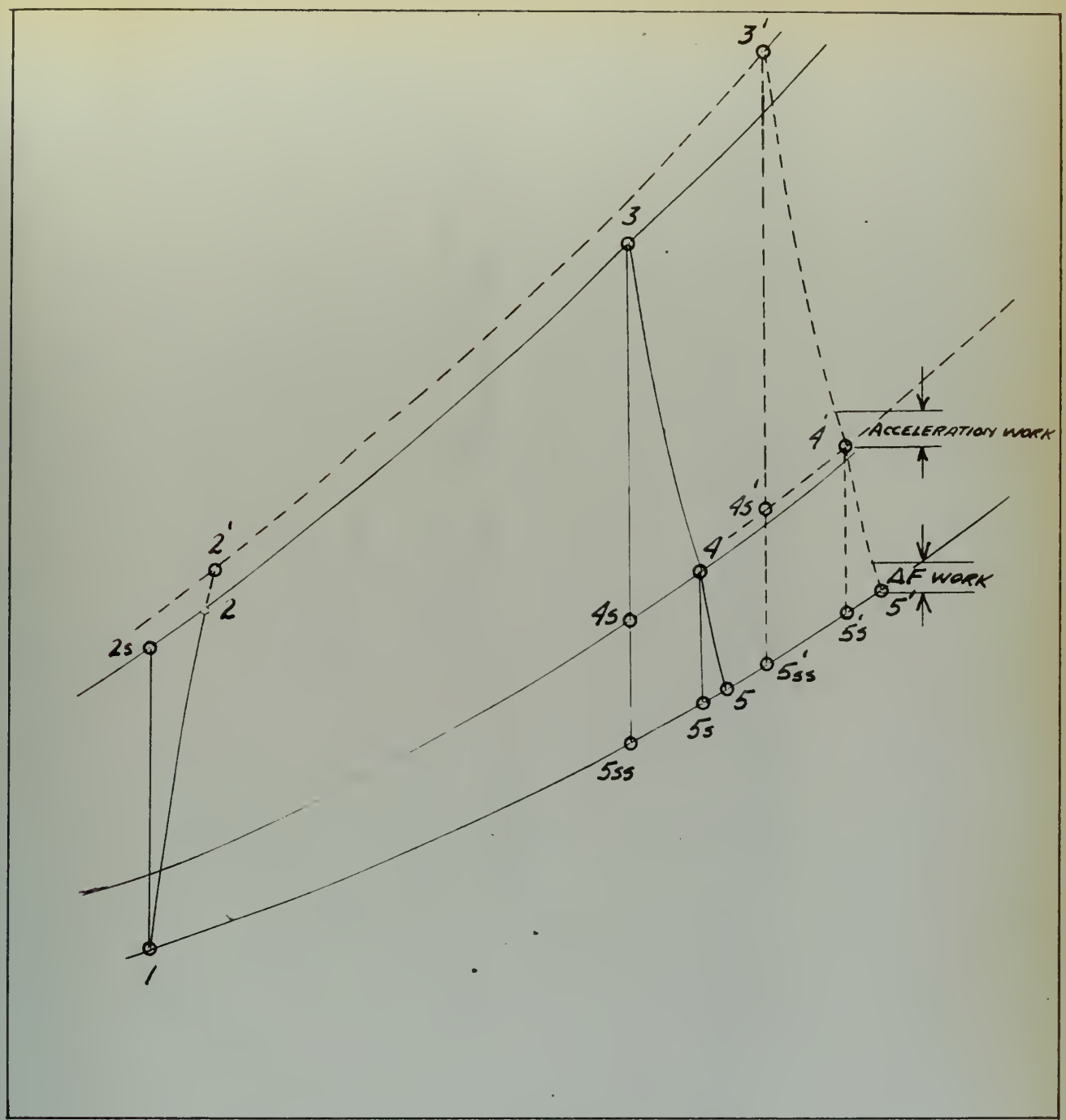

TURBO-JET CYCLE

TRANSIENT OPERATION

FIG. NO. 1

27500 RPM

2.20

26500 RPM

2.10

29000 RPM

TRANSIENT PATH
22000 - 28000 RPM

25500 RPM

1700°R

1600°R

1800°R

27000 RPM

2.00

24500 RPM

1900°R

2000°R

EQUILIBRIUM OPERATING LINE

26000 RPM

PRESSURE RATIO

1.90

23500 RPM

25000 RPM

1.80

22500 RPM

29000 RPM

ENGINE MATCHING CHARACTERISTIC CURVES

CALCULATED AND COMPILED FROM REFERENCES 3 & 9

FIG 2

1.70

23000 RPM

22000 RPM

1.62

3.5 3.6 3.7 3.8 3.9 4.0 4.1 4.2 4.3 4.4 4.5 4.6 4.7 4.8 4.9 5.0 5.1 5.2 5.3 5.4 5.5

Wa - MASS FLOW lbs/sec.

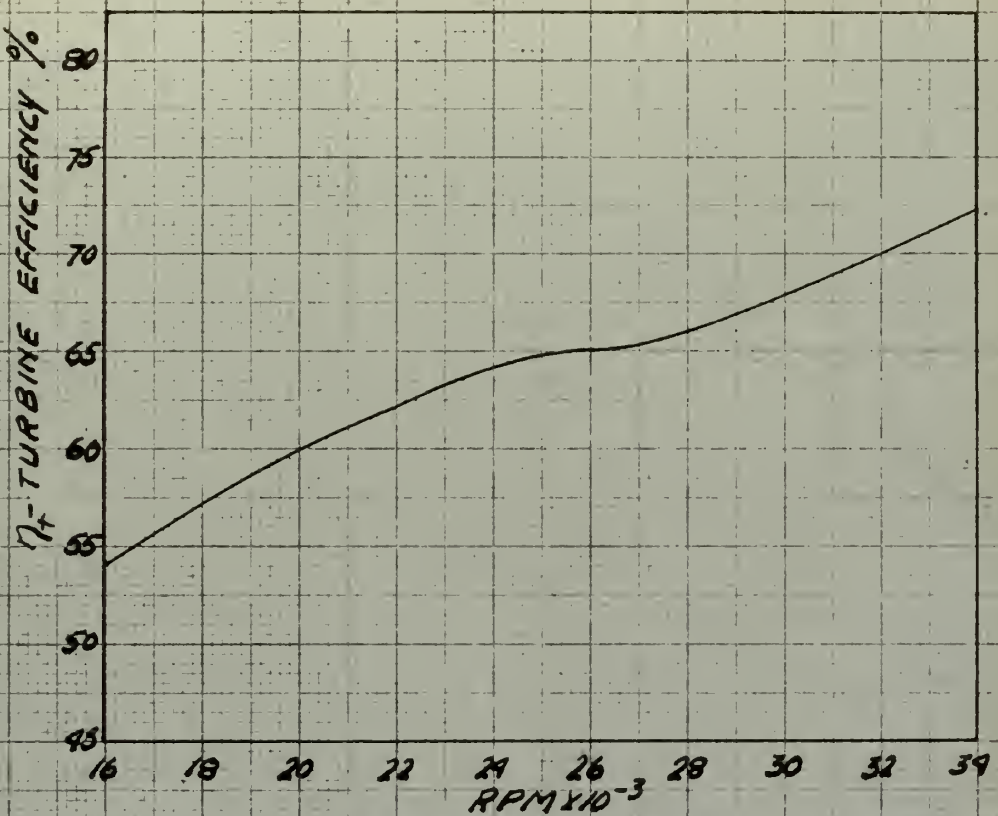

CALCULATED EFFECTIVE TURBINE EFFICIENCY
FIG. NO. 3

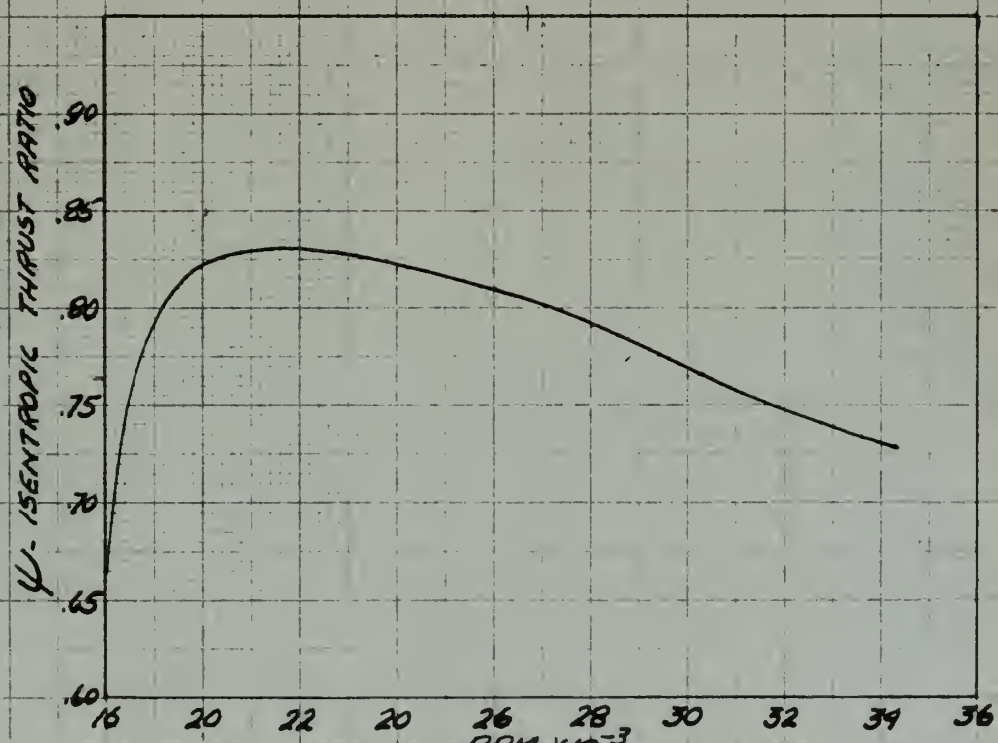

ISENTROPIC THRUST/WORK RATIO
FIG. NO. 4

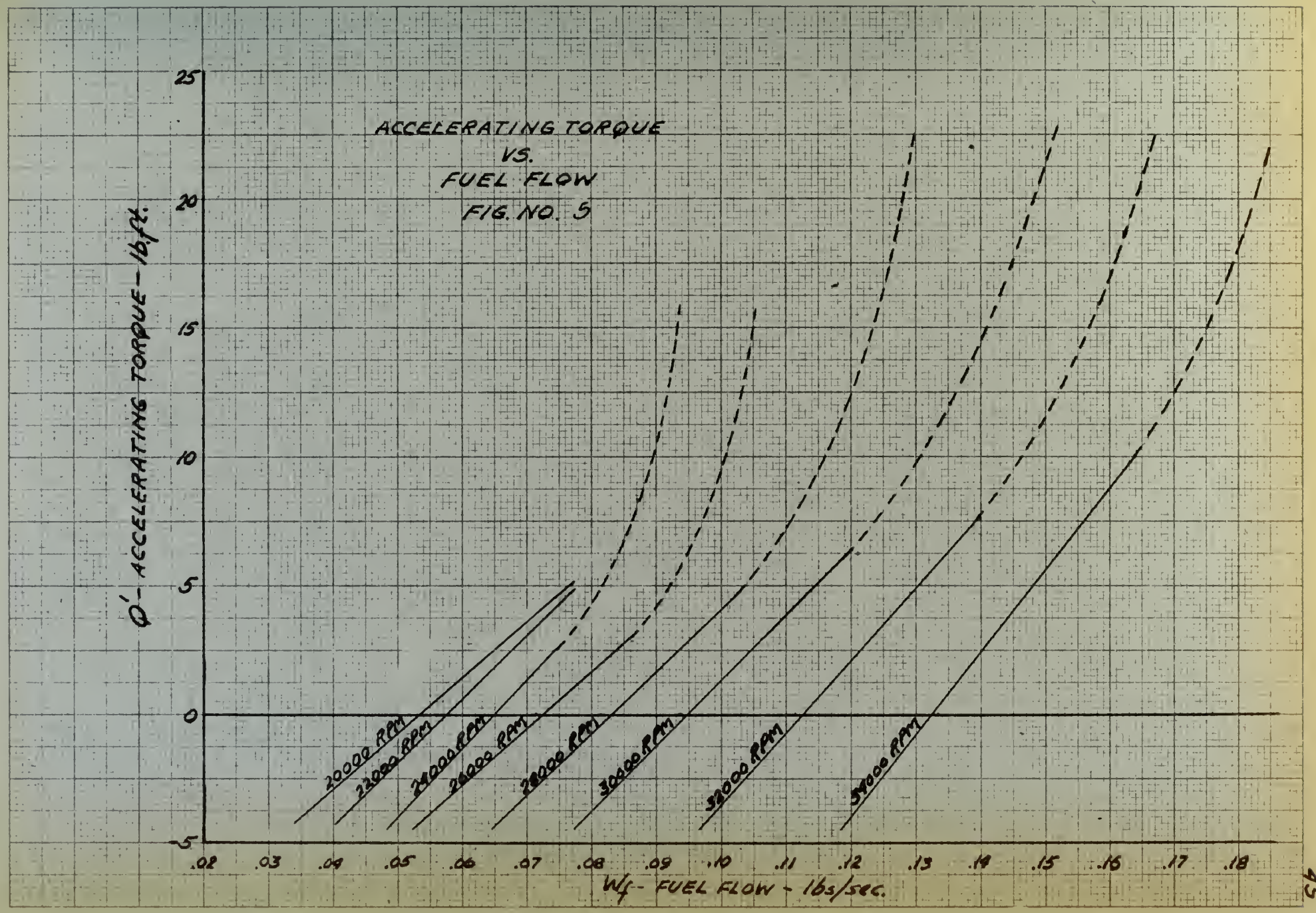
ACCELERATING TORQUE
VS.
FUEL FLOW
FIG. NO. 5
Q' - ACCELERATING TORQUE - lb/ft.
25
20
15
10
5
0
-5
20000 RPM
22000 RPM
24000 RPM
26000 RPM
28000 RPM
30000 RPM
32000 RPM
34000 RPM
.02
.03
.04
.05
.06
.07
.08
.09
.10
.11
.12
.13
.14
.15
.16
.17
.18
Wf - FUEL FLOW - lbs/sec.

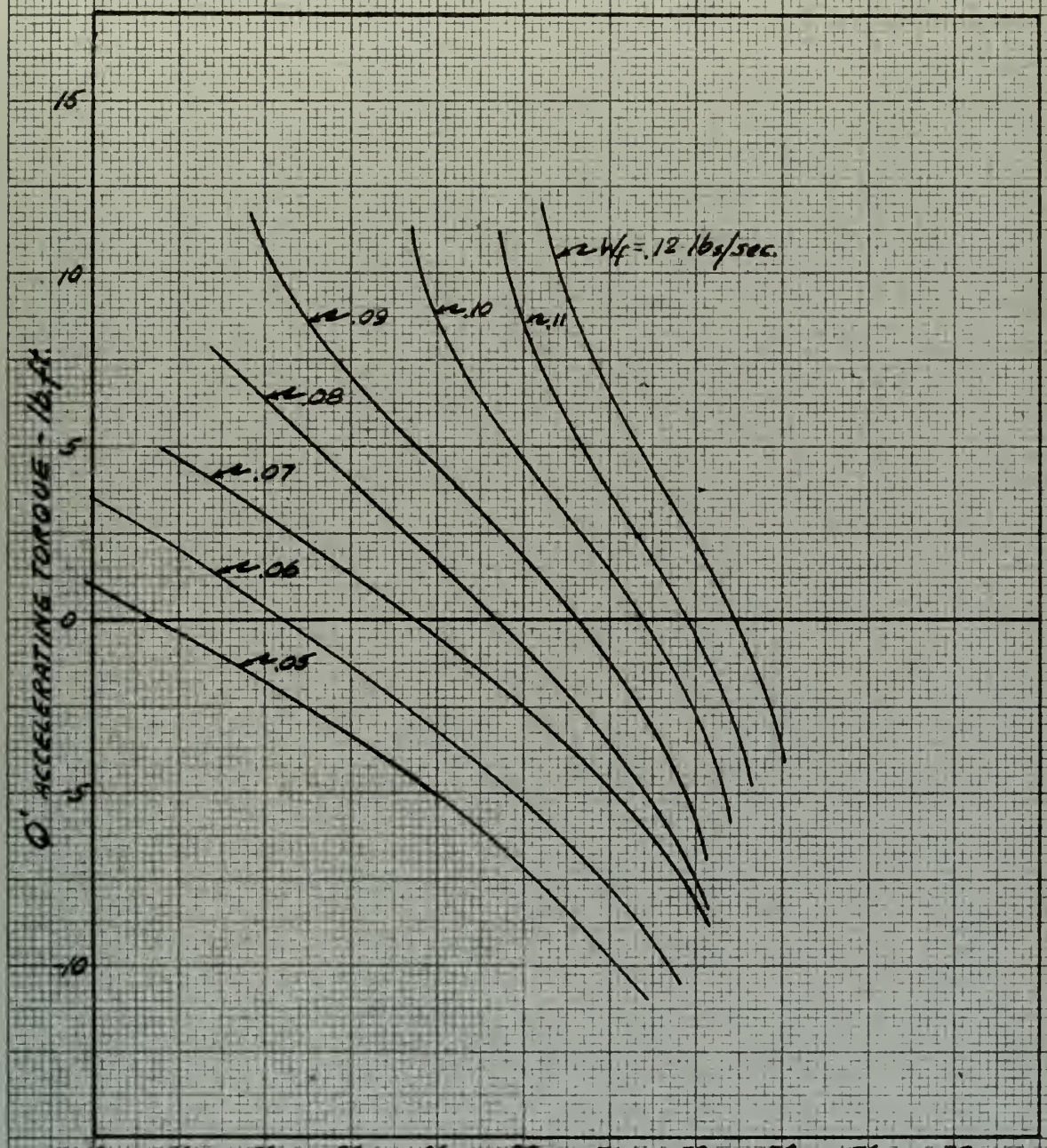

ACCELERATING TORQUE
VS.
RPM
FIG. NO. 6

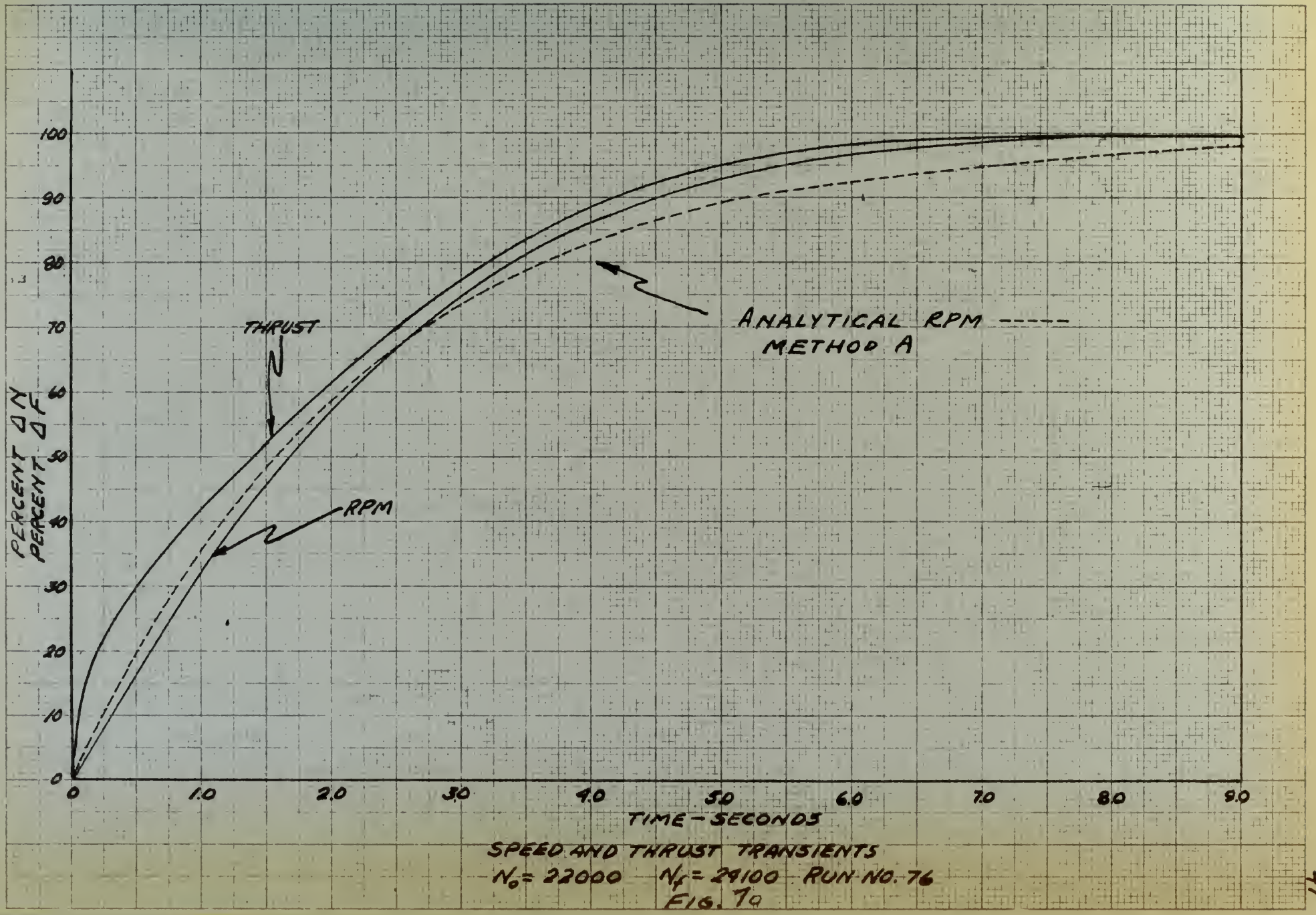

SPEED AND THRUST TRANSIENTS
N_o = 22000 N_f = 29100 RUN NO. 76
FIG. 7o

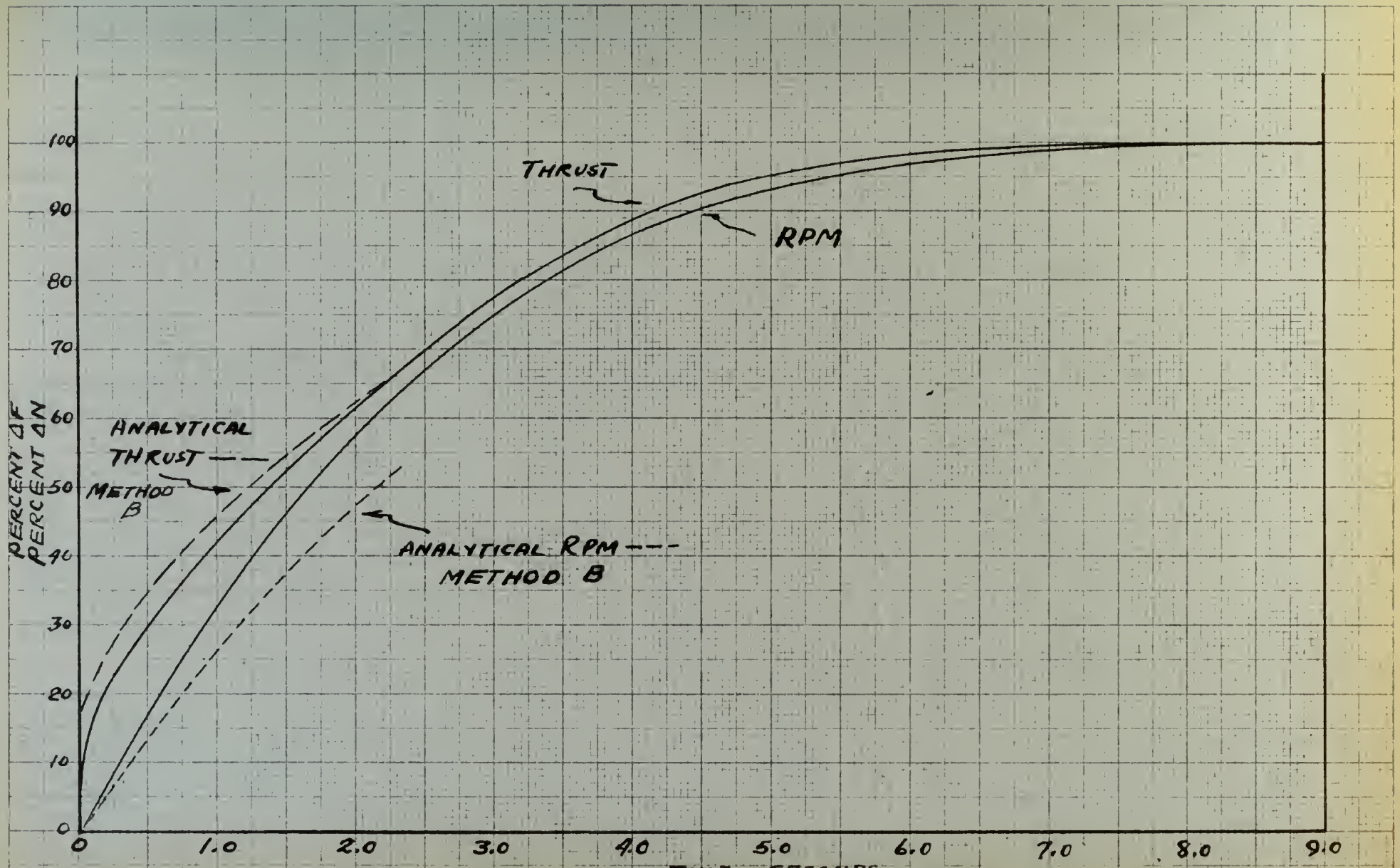

SPEED AND THRUST TRANSIENTS

$N_0 = 22,000$ $N_f = 24,100$ RUN NO 76

FIG 76

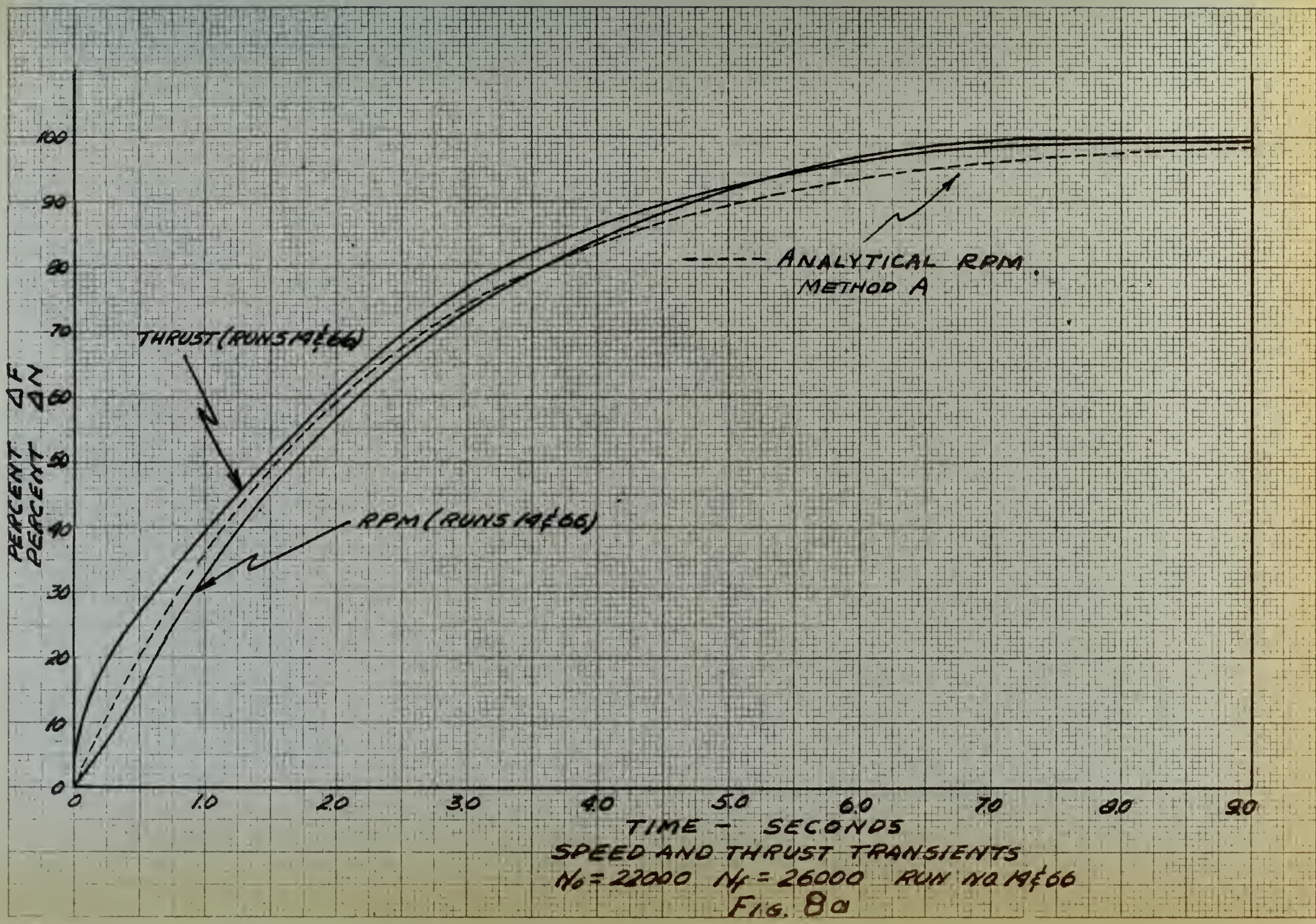

SPEED AND THRUST TRANSIENTS

$N_0 = 22000$ $N_f = 26000$ RUN NO 19 & 66

FIG. 8a

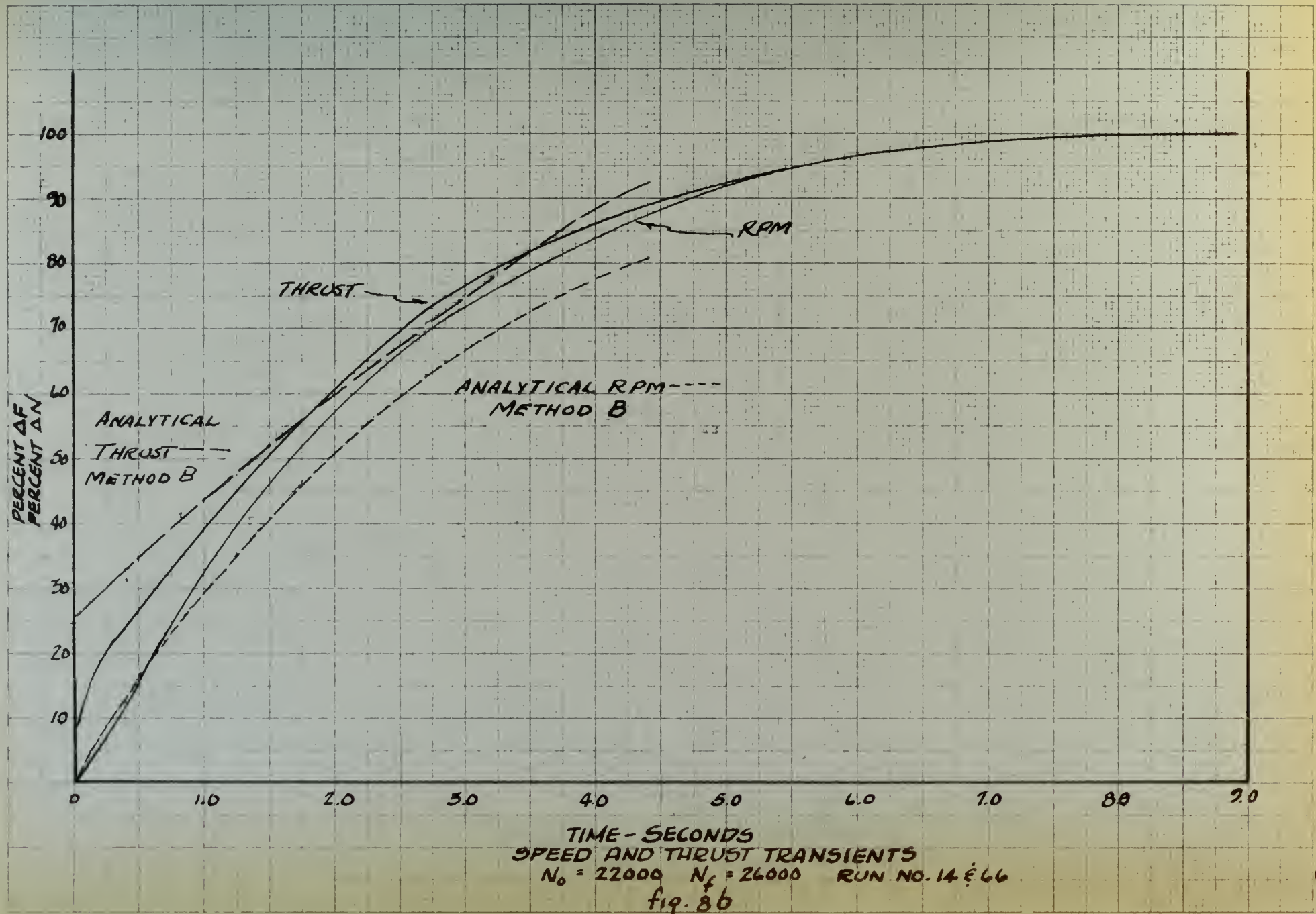

SPEED AND THRUST TRANSIENTS
N_o = 22000 N_f = 26000 RUN NO. 14 & 66

fig. 86

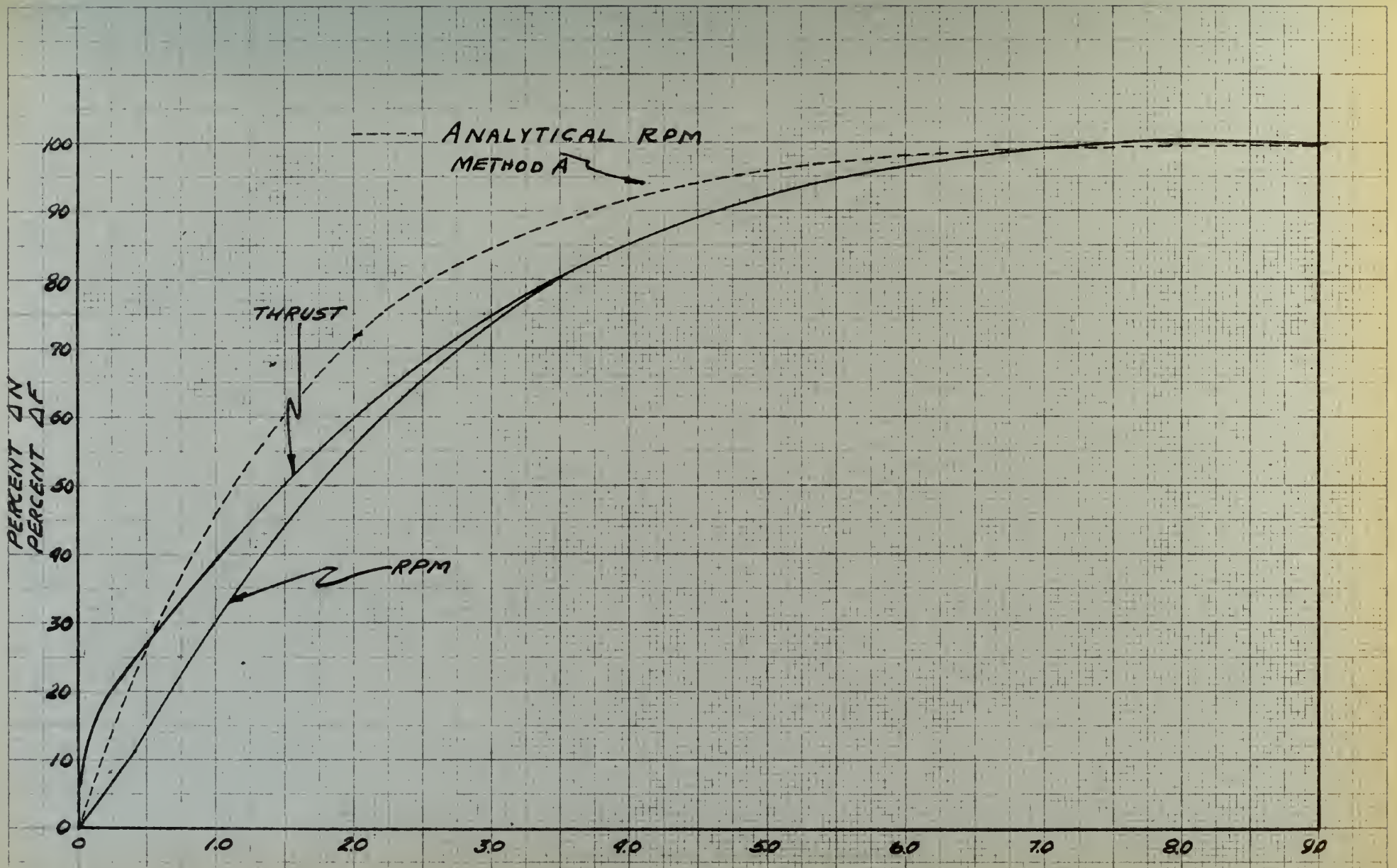

SPEED AND THRUST TRANSIENTS
$N_0 = 22000$ $N_f = 28000$ RUN NO. 68
FIG. 9a

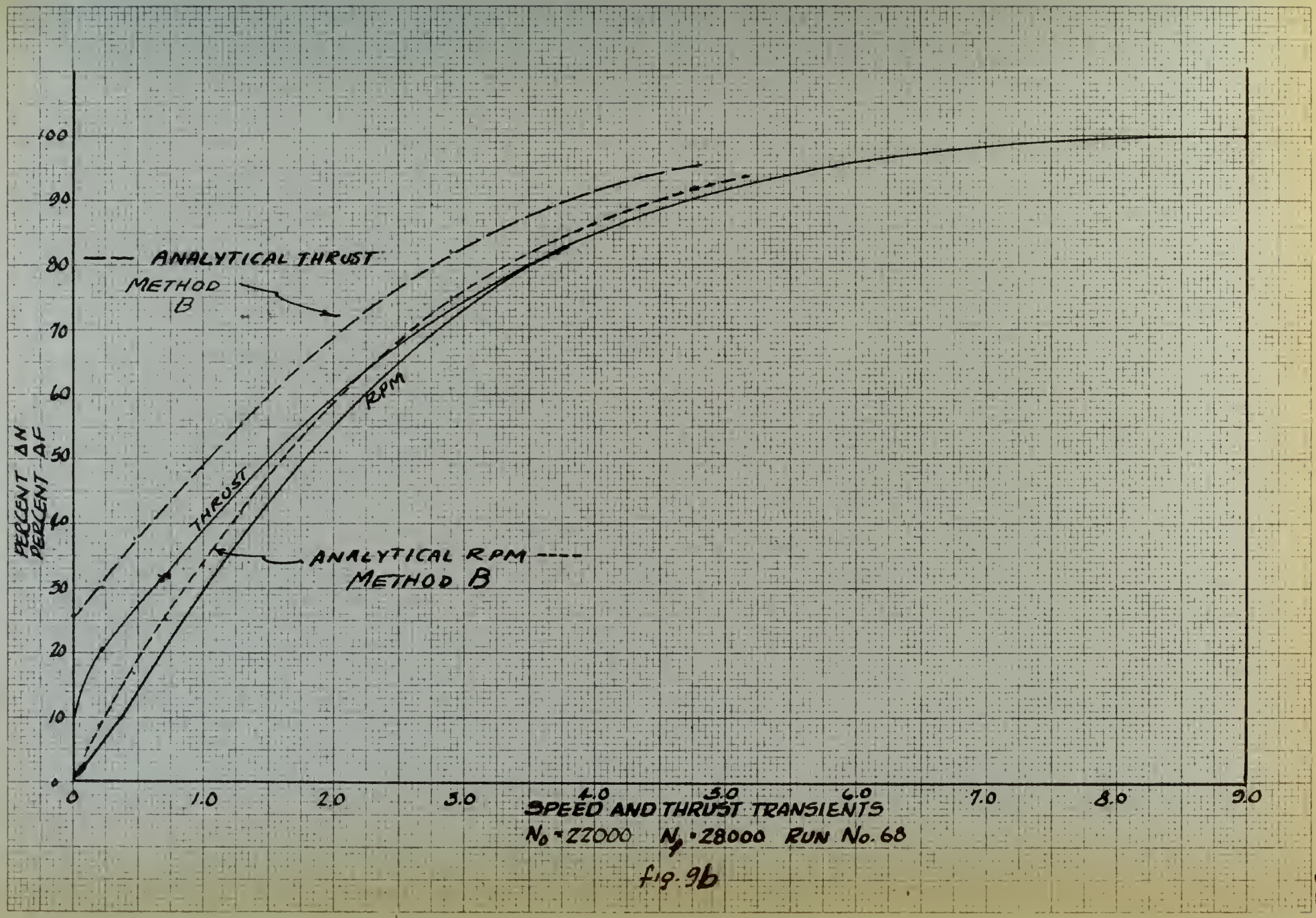

SPEED AND THRUST TRANSIENTS

N_0 = 22000 N_f = 28000 RUN No. 68

fig. 9b

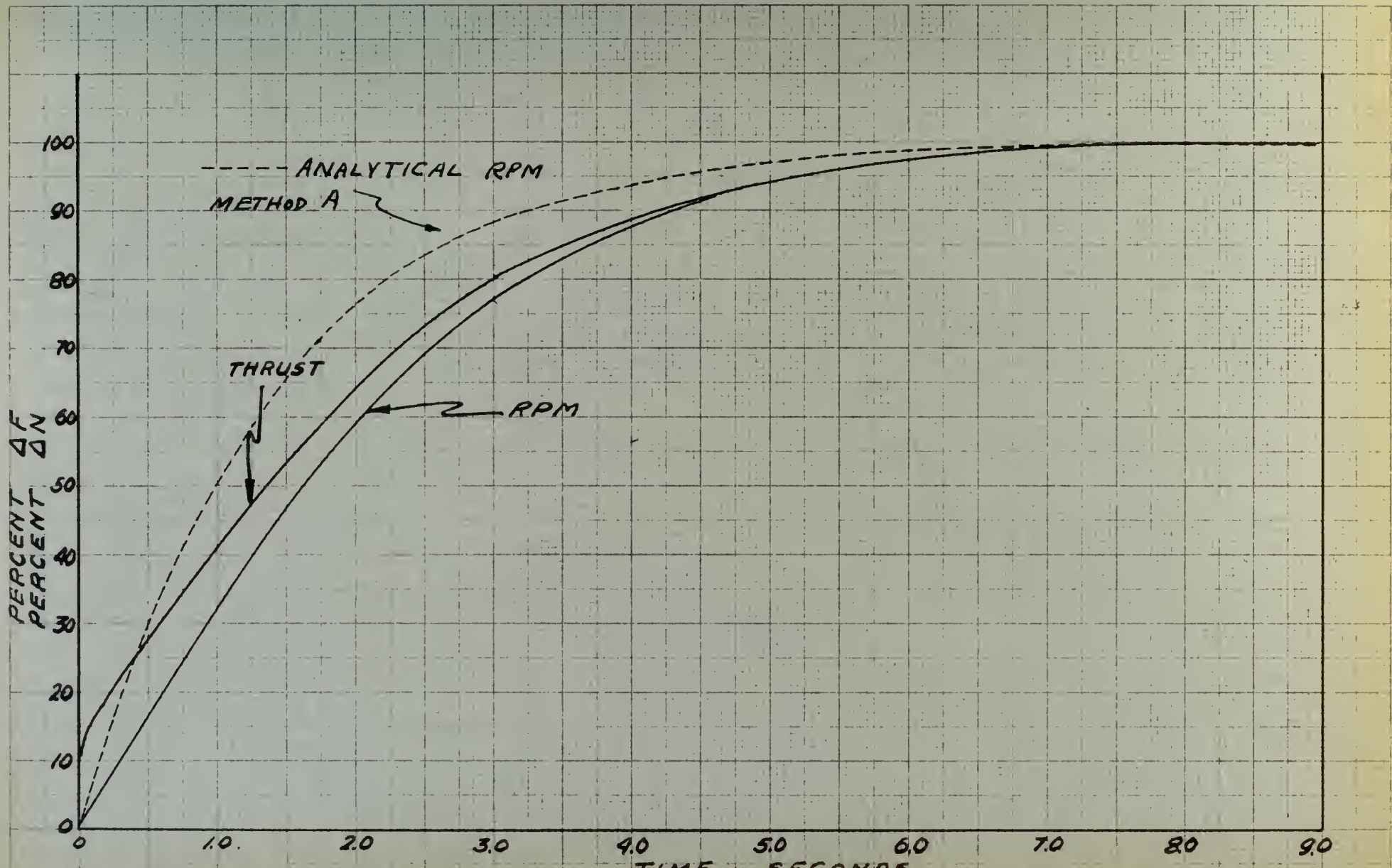

SPEED AND THRUST TRANSIENTS
$N_0 = 22000$ $N_f = 29,750$ RUN No 73

FIG. 10

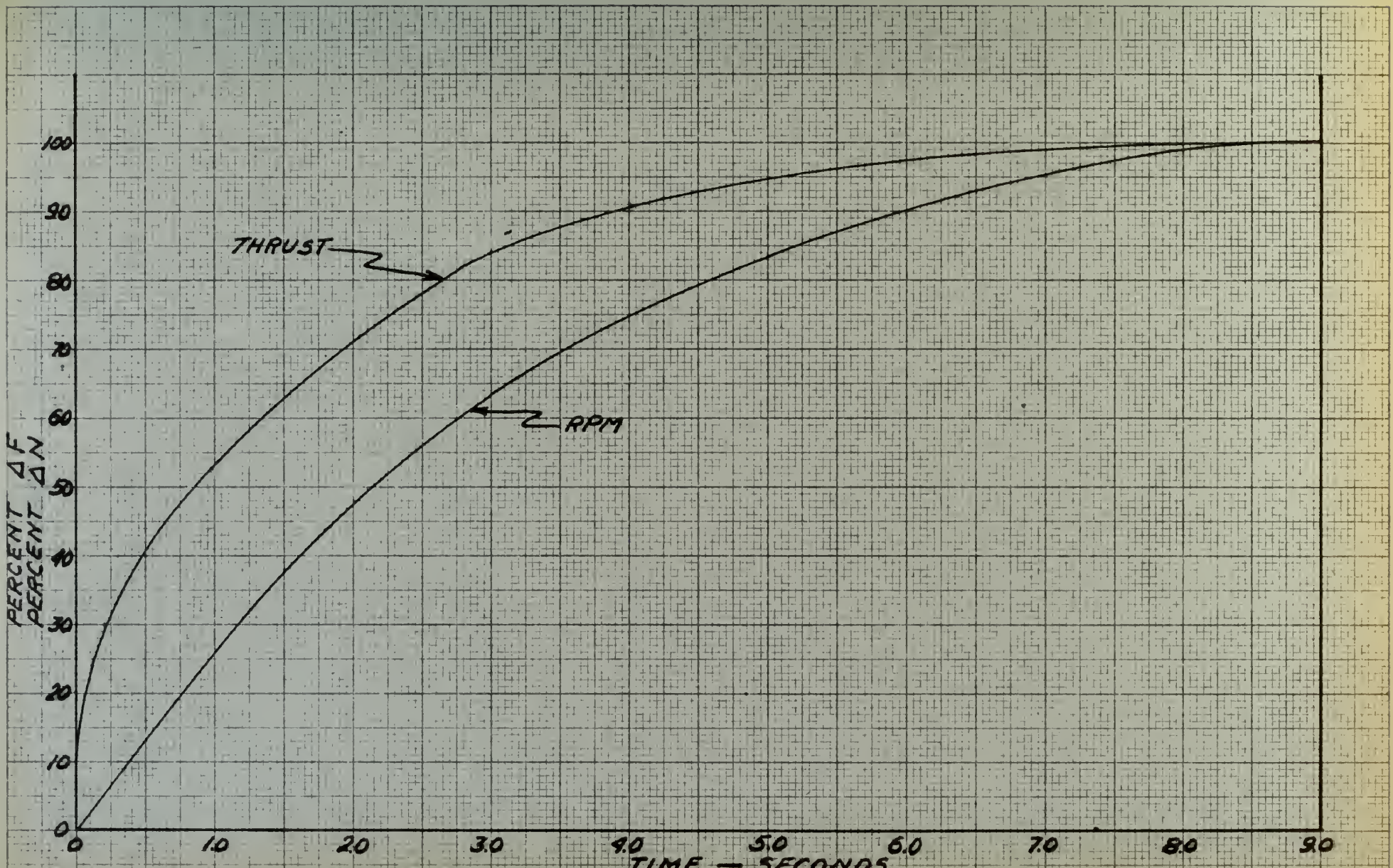

SPEED AND THRUST TRANSIENTS

$N_o = 29000$ $N_f = 22000$ RUN NO. 57

FIG. 11a

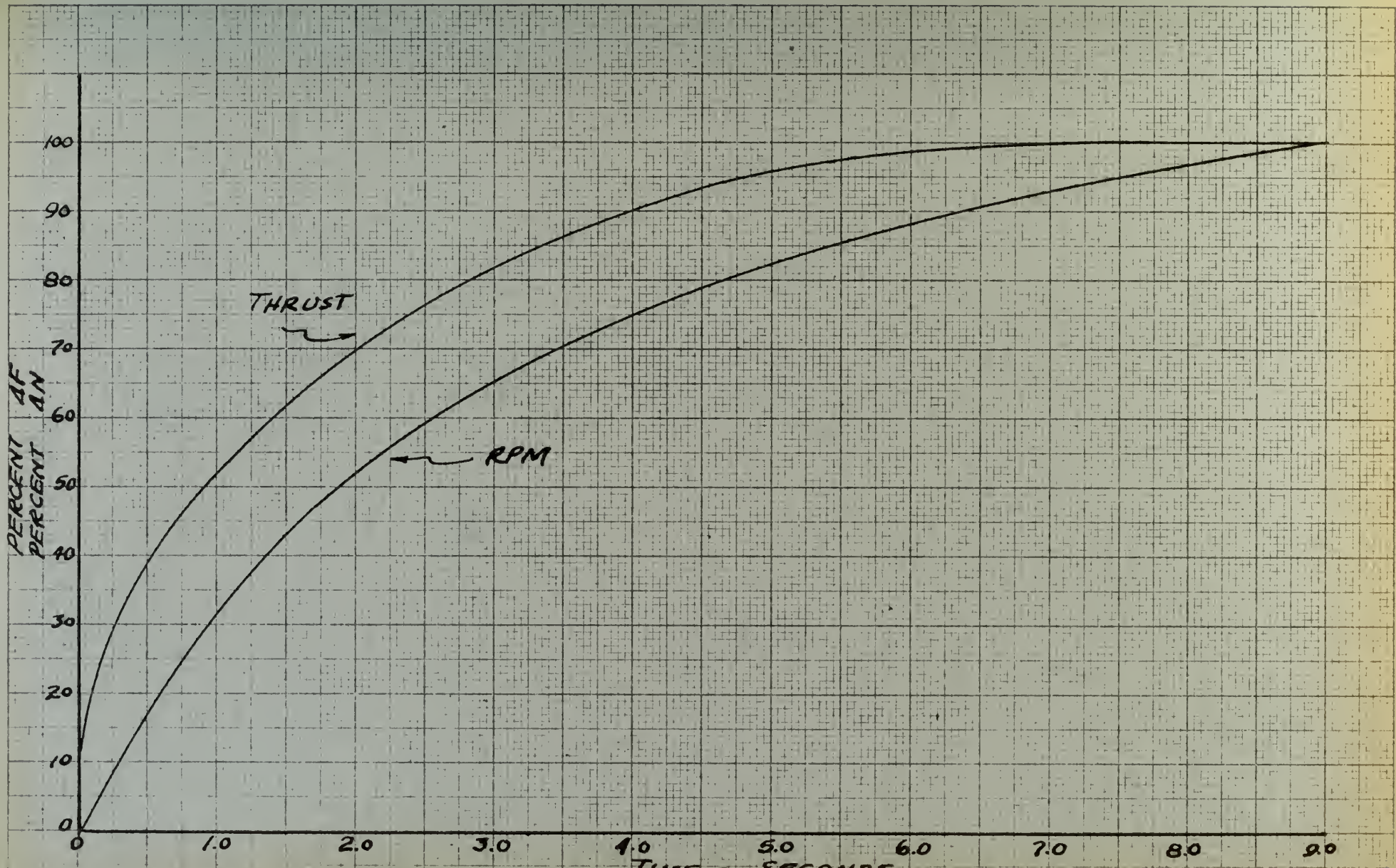

SPEED AND THRUST TRANSIENTS

$N_o = 26{,}000$ $N_f = 22{,}000$ RANGE

FIG. 12a

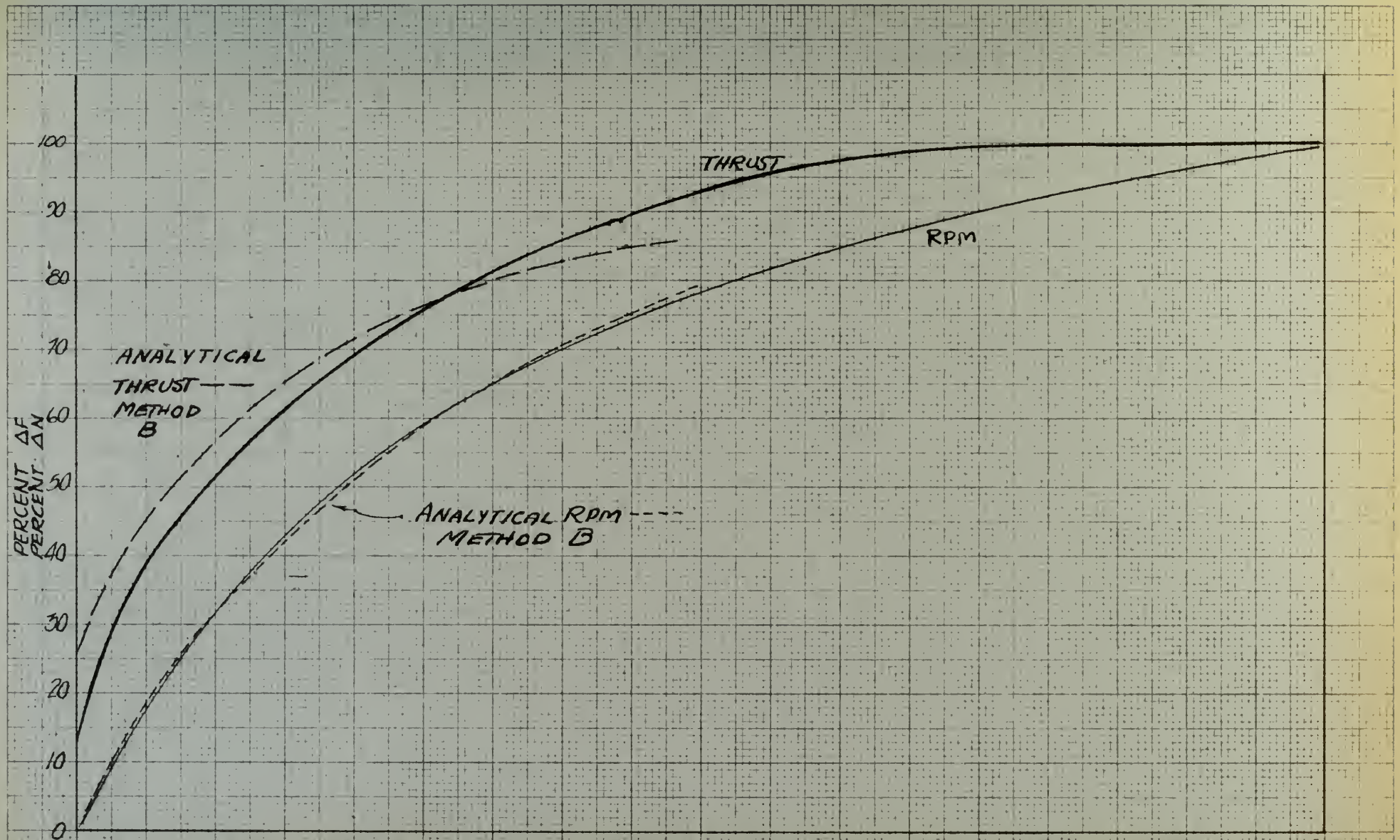

SPEED AND THRUST TRANSIENTS

N_0= 26000 N_f = 22000

fig. 12b.

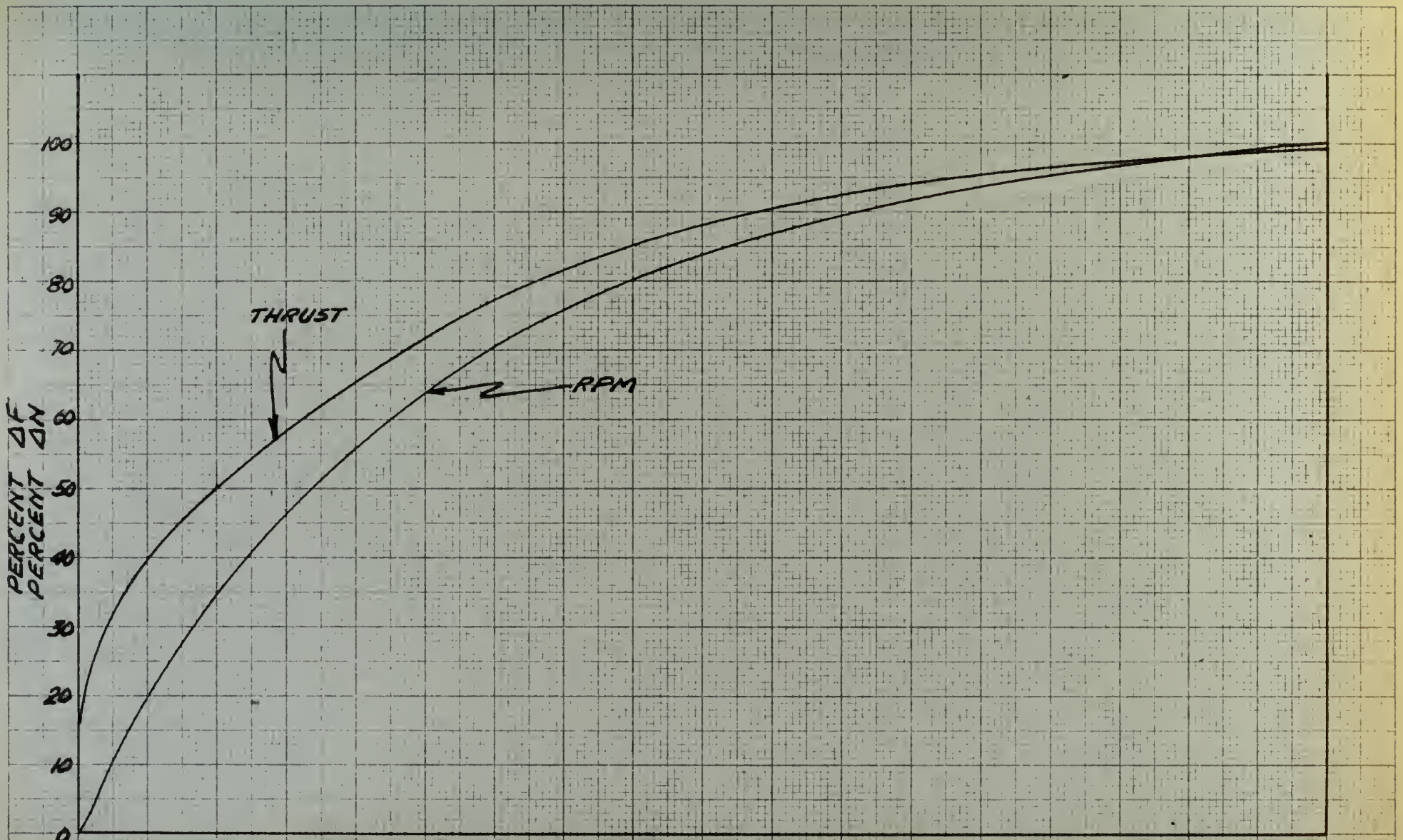

SPEED AND THRUST TRANSIENTS
N_0 = 28000 N_f = 22100 RUN NO. 69

FIG. 13

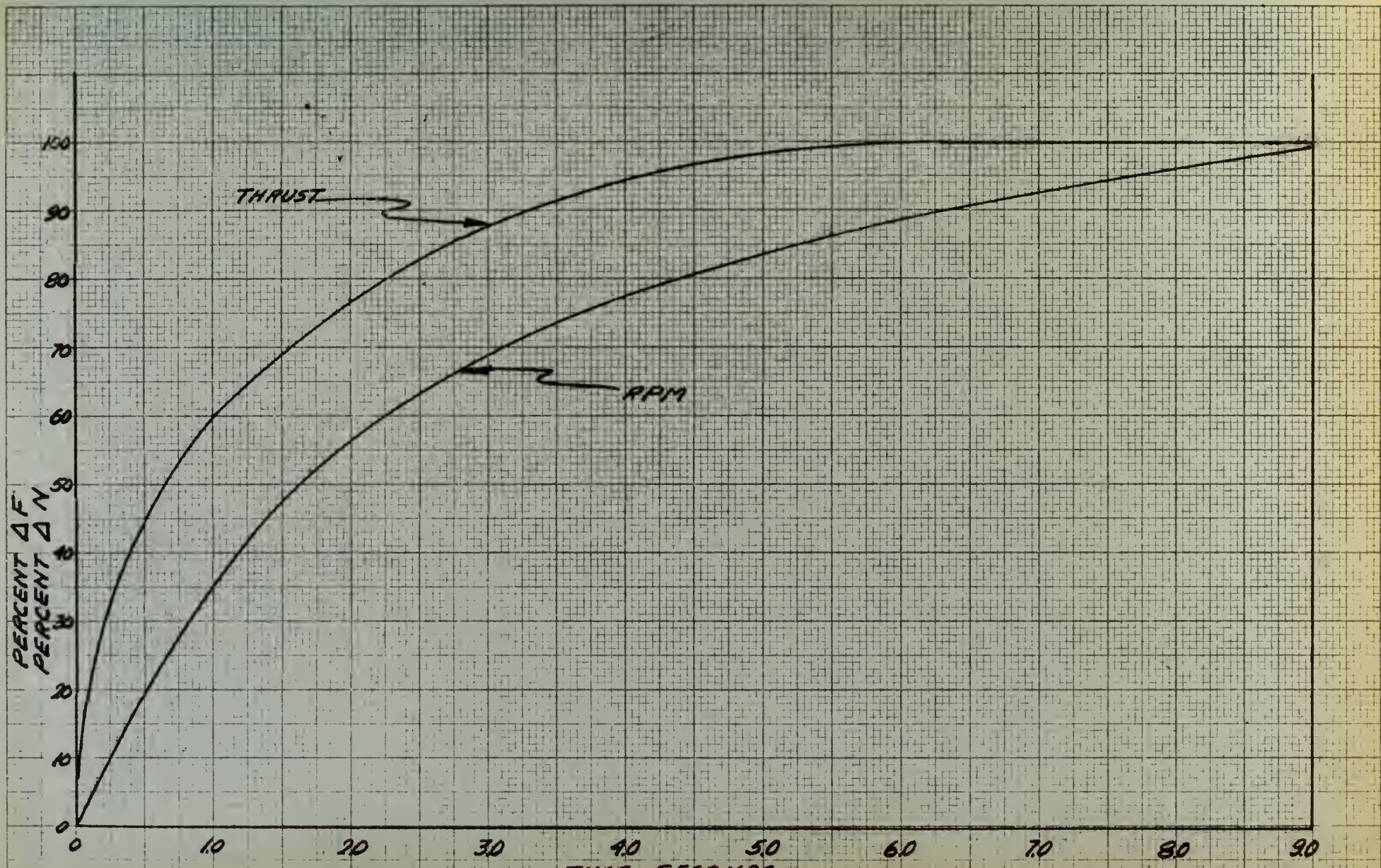

SPEED AND THRUST TRANSIENTS
N_o = 29800 N_f = 21700 RUN 72
FIG. 14

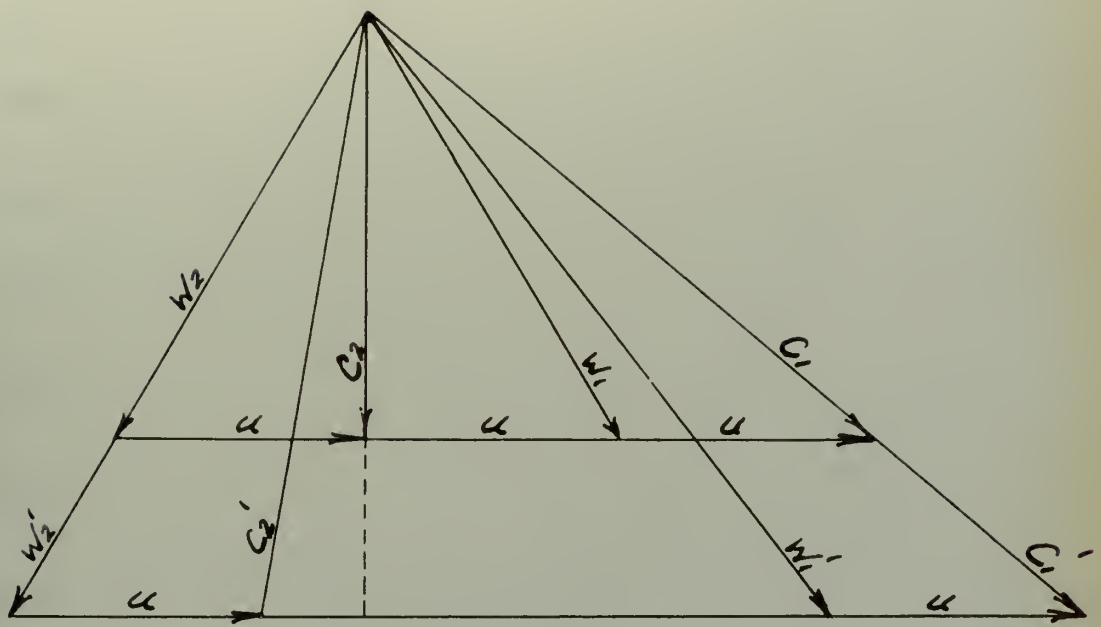

VELOCITY TRIANGLE
FOR
AXIAL FLOW IMPULSE TURBINE
UNDER TRANSIENT OPERATION
FIG. NO. 15

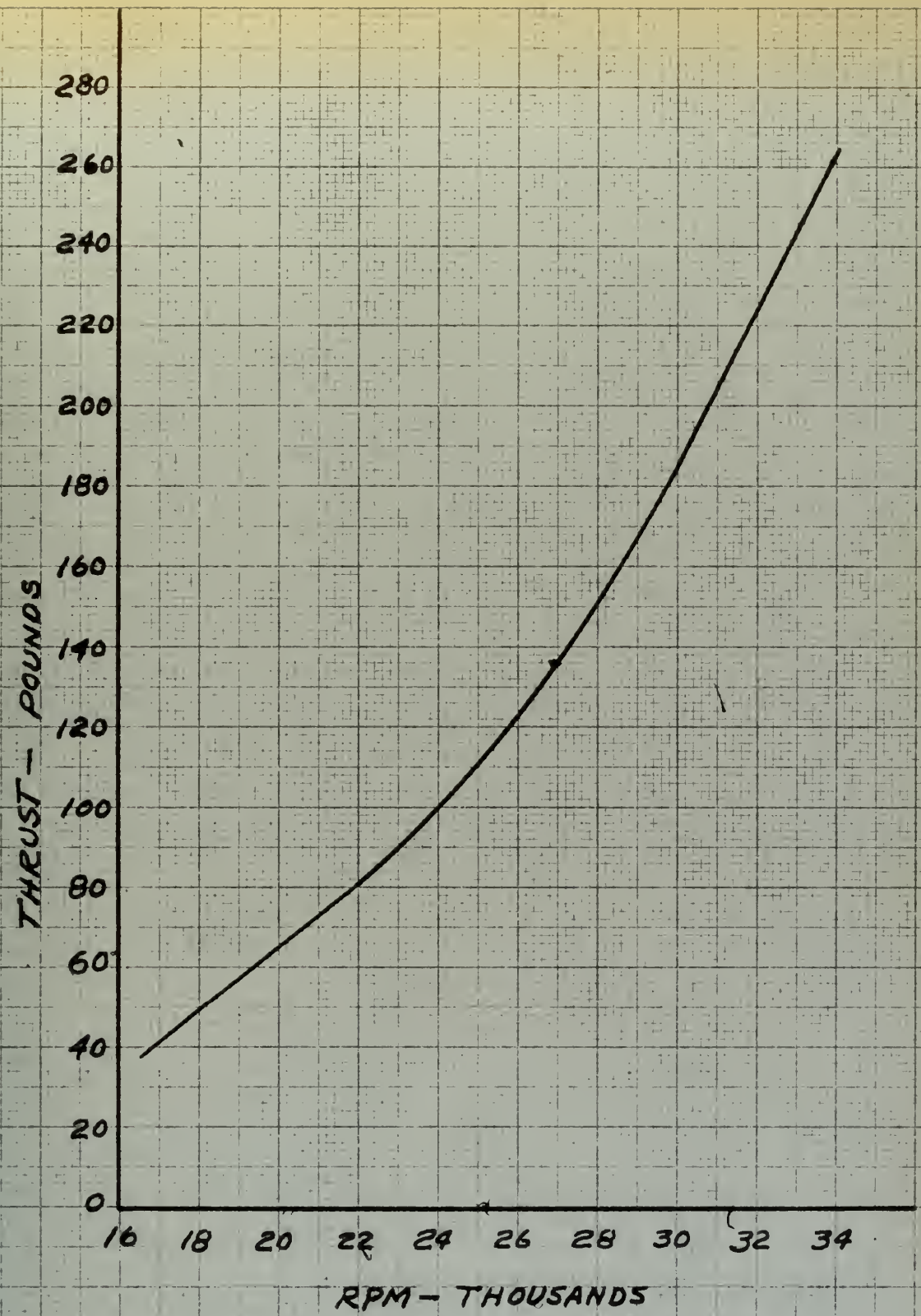

NET THRUST
XJ-32 TURBO JET
FIG. 16

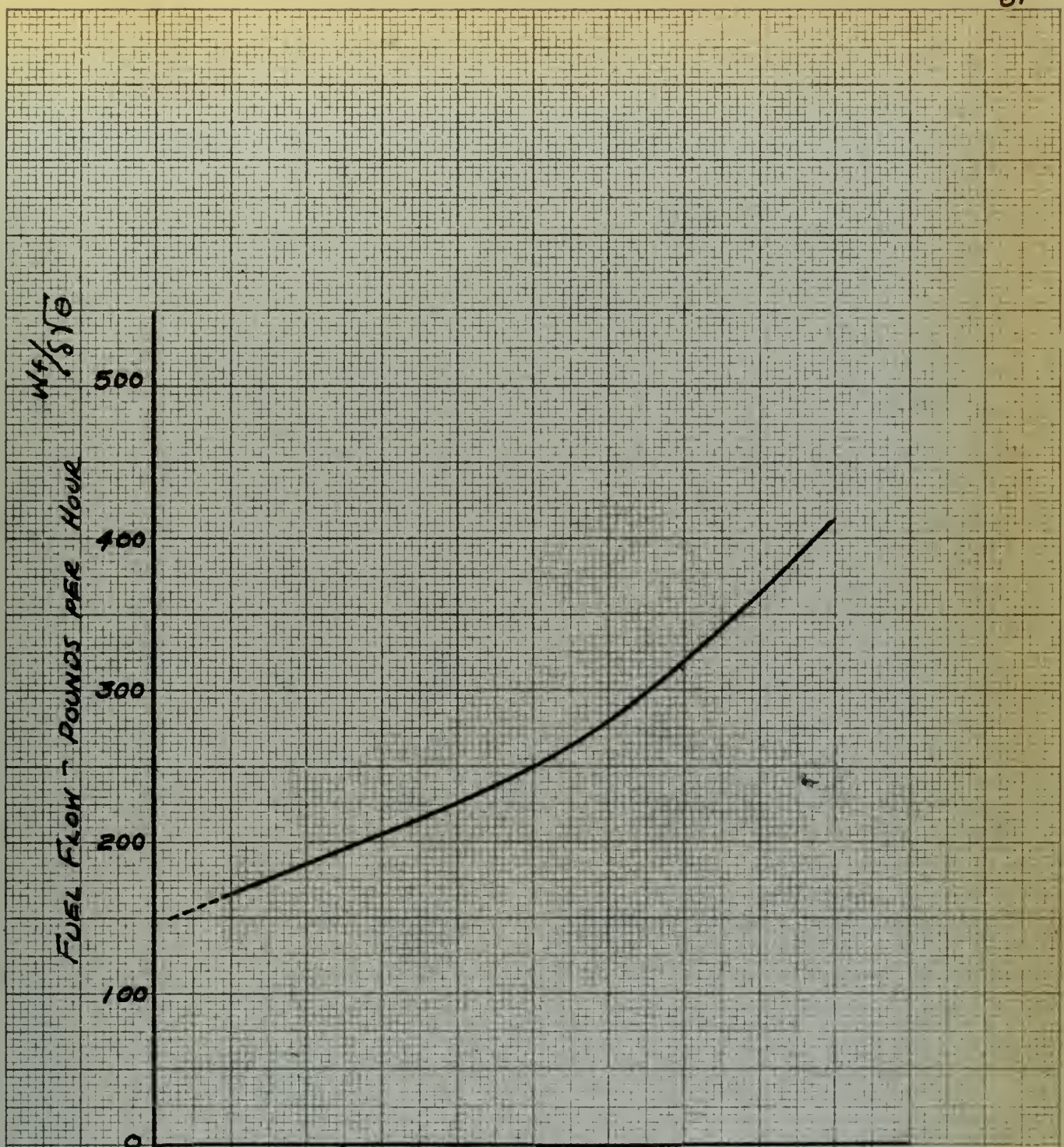

FUEL FLOW
XJ-32-WE-4 TURBO JET

Fig. 16a

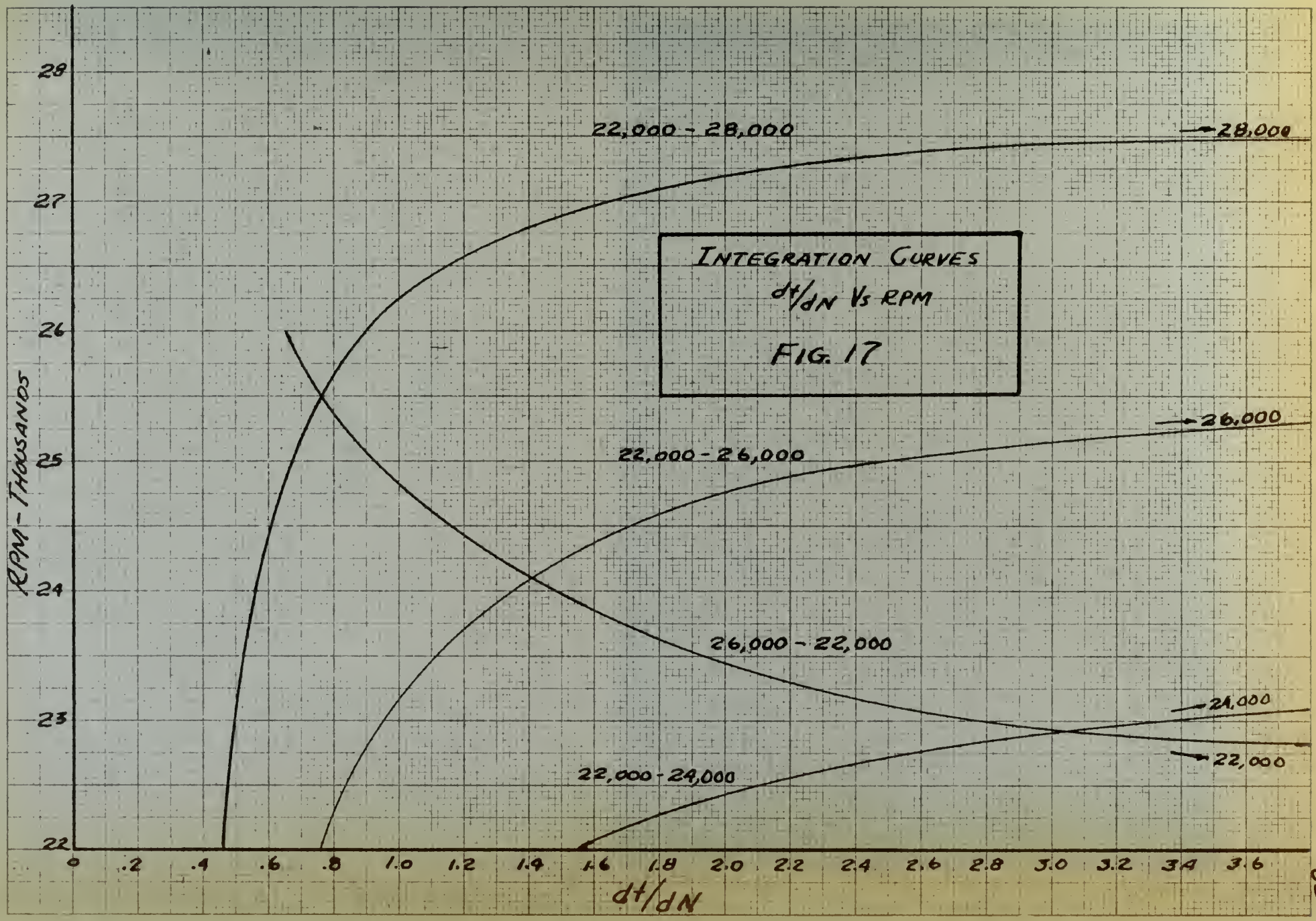
INTEGRATION CURVES
dt/dN Vs RPM
FIG. 17
22,000 - 28,000
28,000
26,000
22,000 - 26,000
26,000 - 22,000
24,000
22,000
22,000 - 24,000
RPM - THOUSANDS
28
27
26
25
24
23
22
0
.2
.4
.6
.8
1.0
1.2
1.4
1.6
1.8
2.0
2.2
2.4
2.6
2.8
3.0
3.2
3.4
3.6
dt/dN

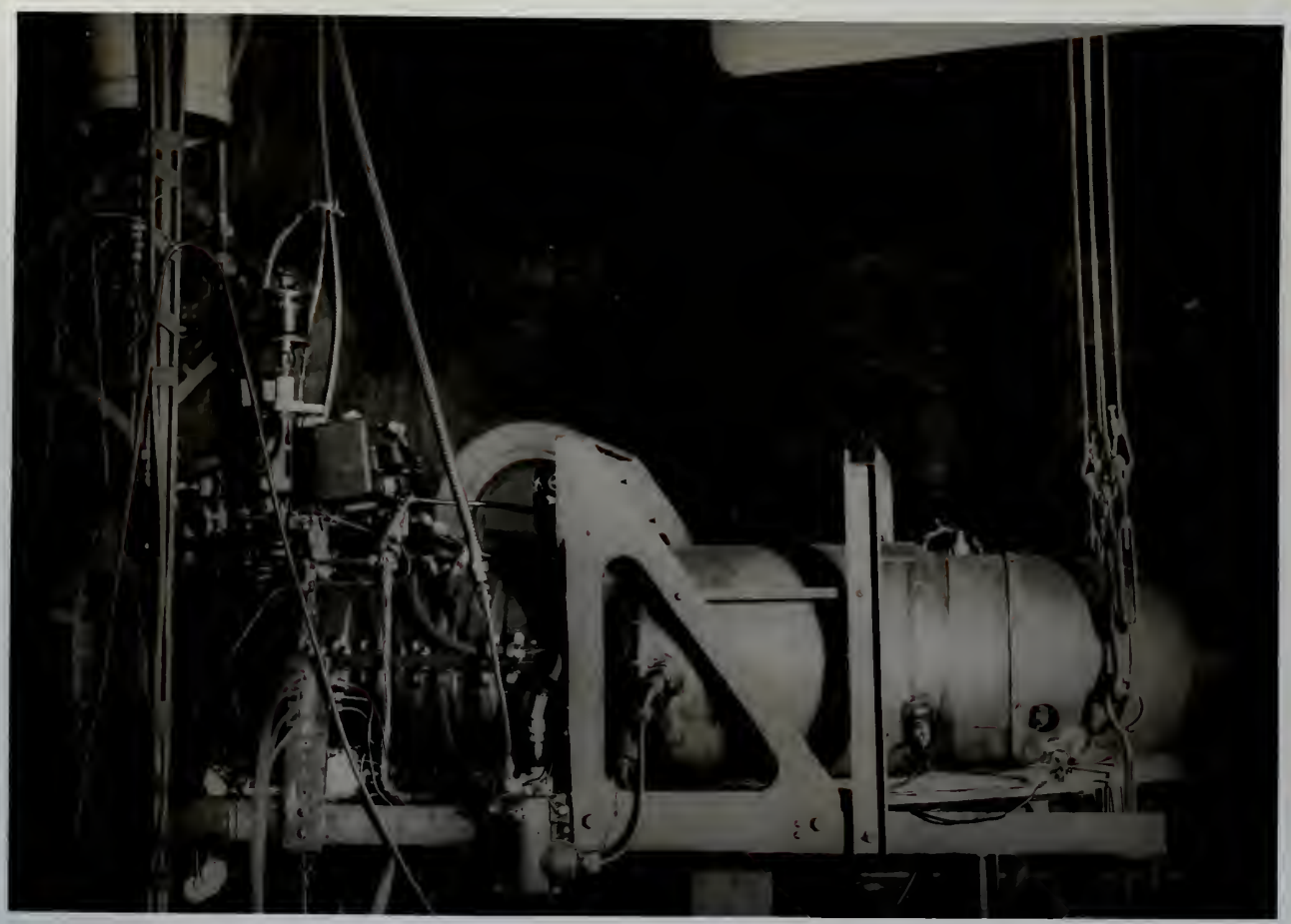

Fig. 18

SIDE VIEW

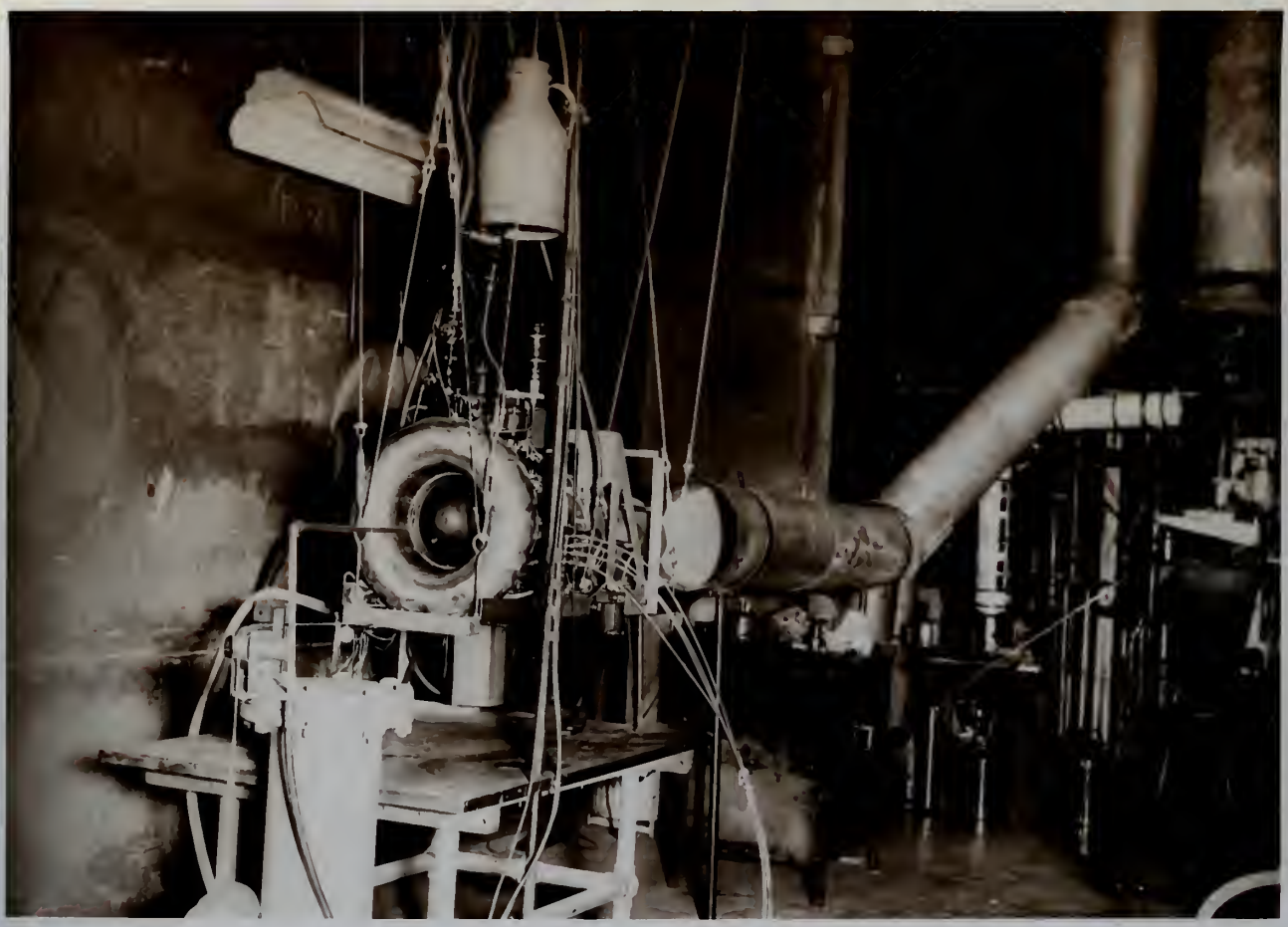

Fig. 19

FRONT VIEW

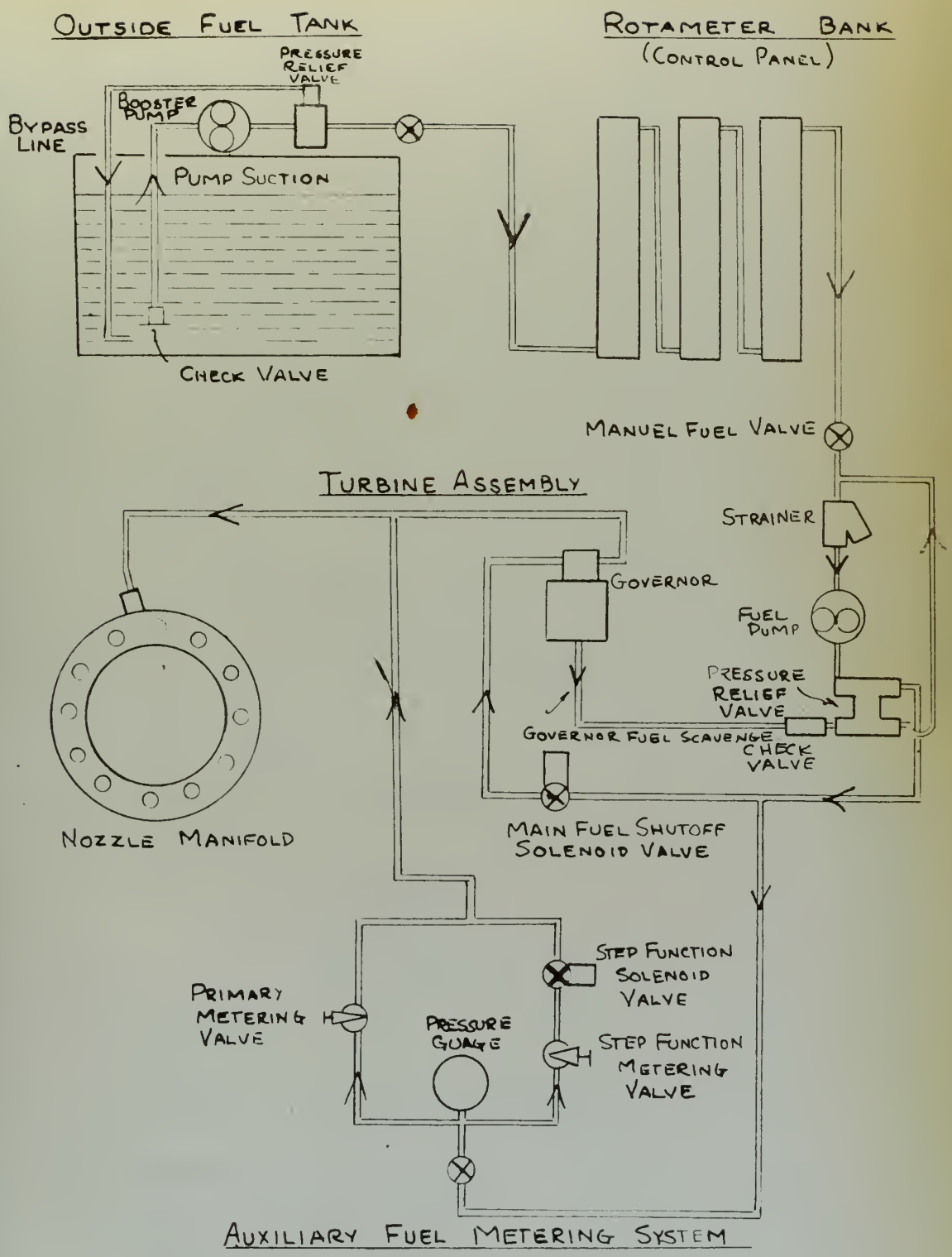

FUEL SYSTEM

X9.5 GAS TURBINE

FIG. 20

TO 60 CONDUCTOR T & T CABLE

1	RED & BROWN
2	BLK. & GREEN
3	RED & TAN
4	RED
5	PINK
6	BLUE
7	BUFF
8	BLACK
9	BUFF
10	RED
11	YELLOW
12	RED
13	PURPLE
14	RED
15	GREY
16	BLK. & GREY
17	BLK. & YELLOW
18	BLK. & BROWN
19	BLK & BLUE
20	RED & GREEN
21	RED & ORANGE
22	RED & BLUE
23	BUFF & GREEN
24	BLACK
25	PURPLE
26	BLACK
27	RED
28	BUFF PINK BLACK & LT. BL.

TERMINAL BOARD

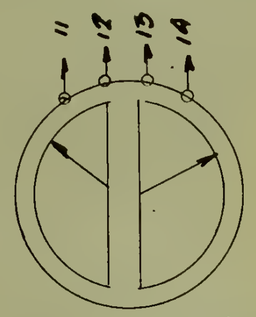

NO. 1 BRG.

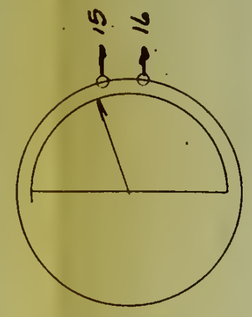

NO. 2 BRG

NO. 3 BRG.

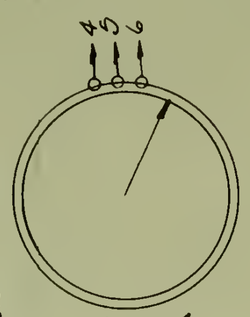

RPM

TO GALVANOMETER

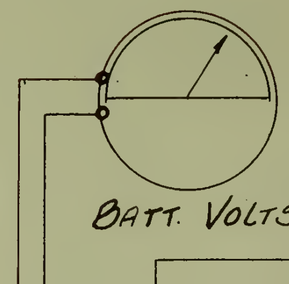

BATT. VOLTS

110 V D.C.

CHARGE

15 amp. fuzes

60 Ω

BATT. ON

OPEN

OFF

CLOSE

STEP FUEL

VOLT. IND.

GALVE SIGN

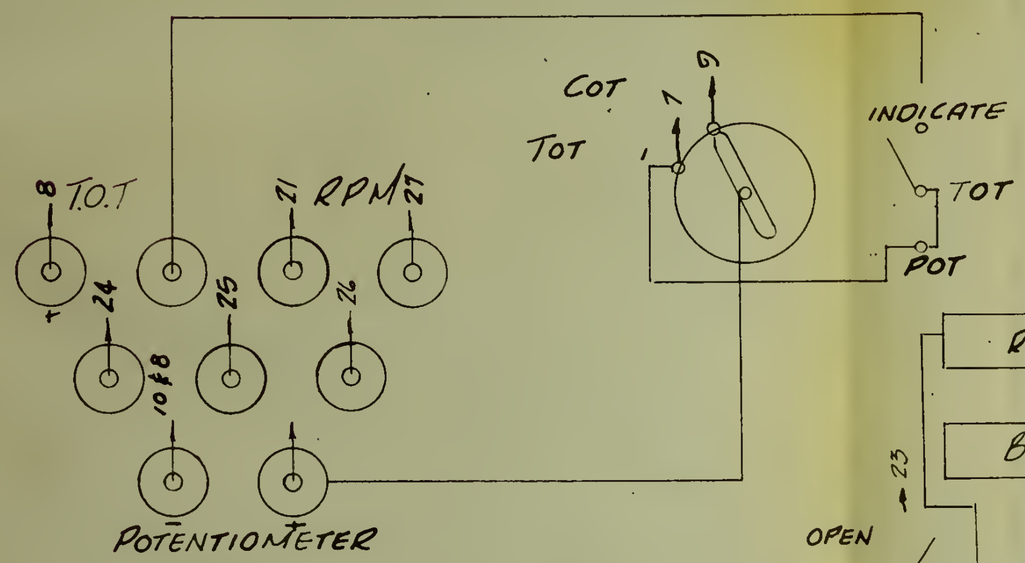

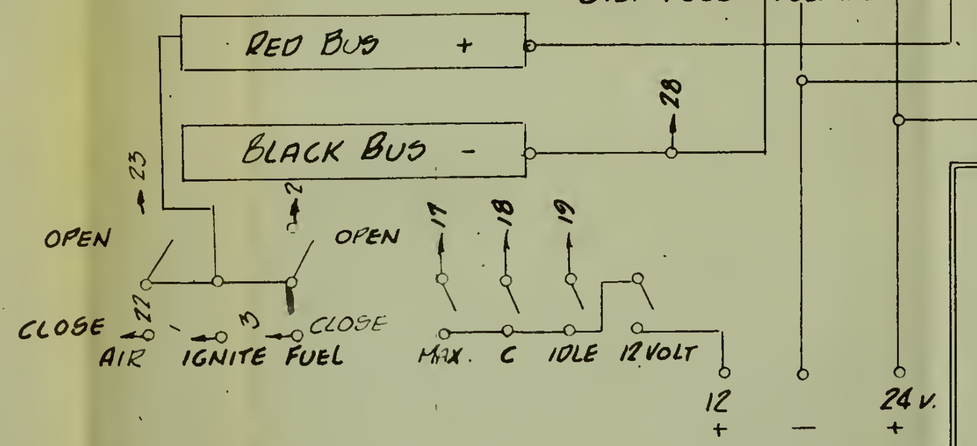

WIRING DIAGRAM FOR TURBO-JET CONTROL PANEL

fig. no. - 21

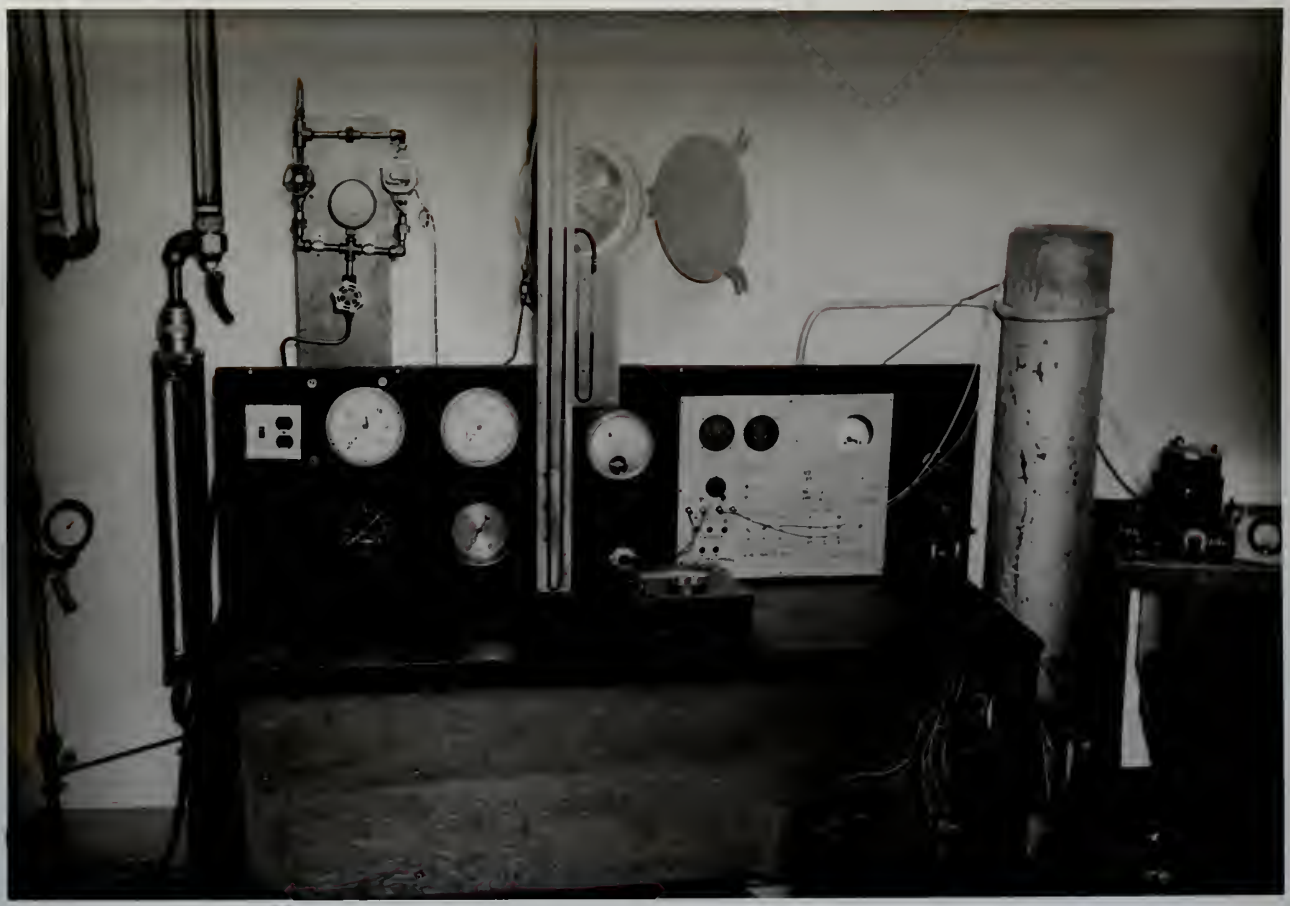

Fig. 22

CONTROL PANEL

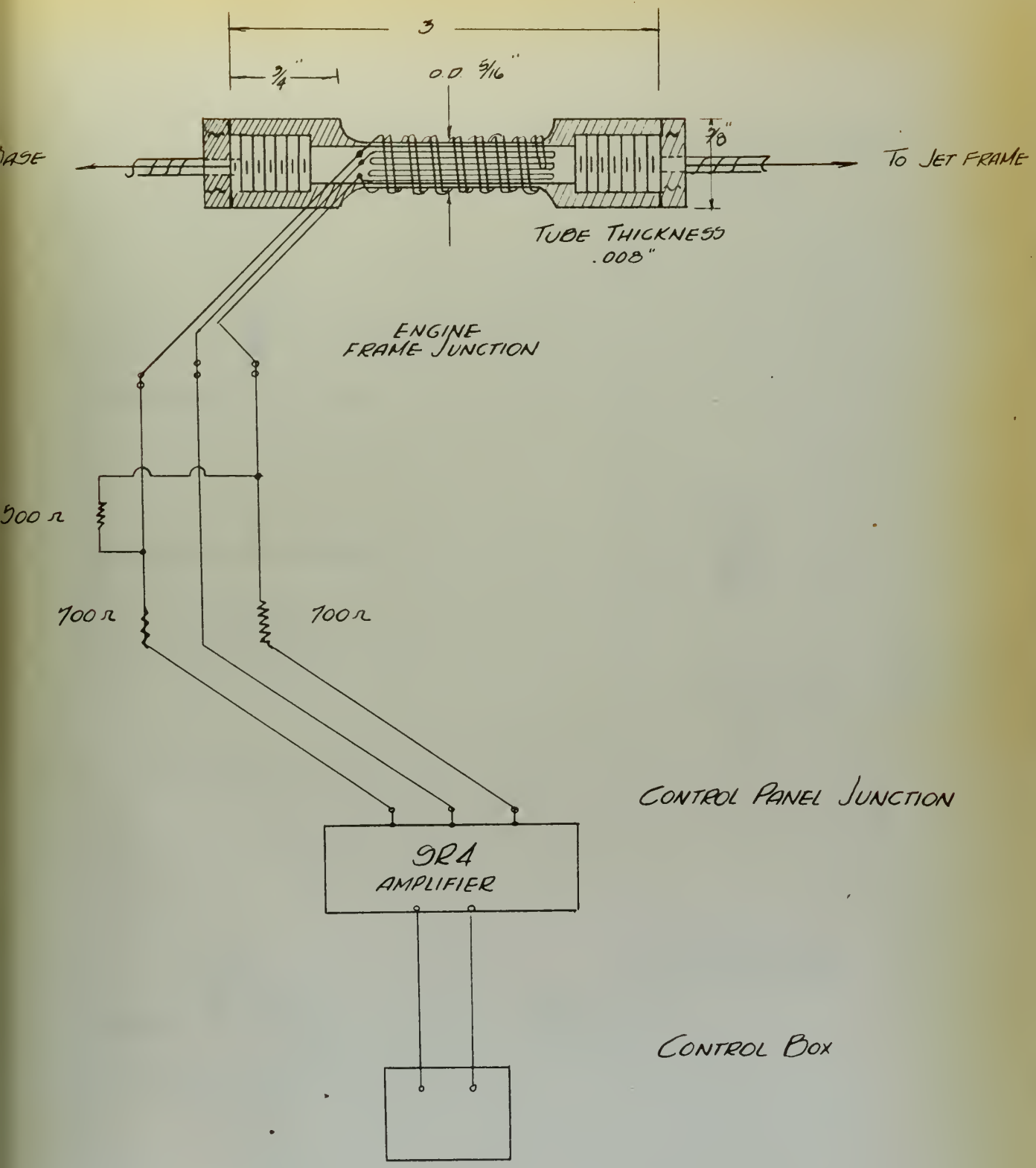

STRAIN GAGE AND THRUST MEASUREMENT SYSTEM

fig no. 23

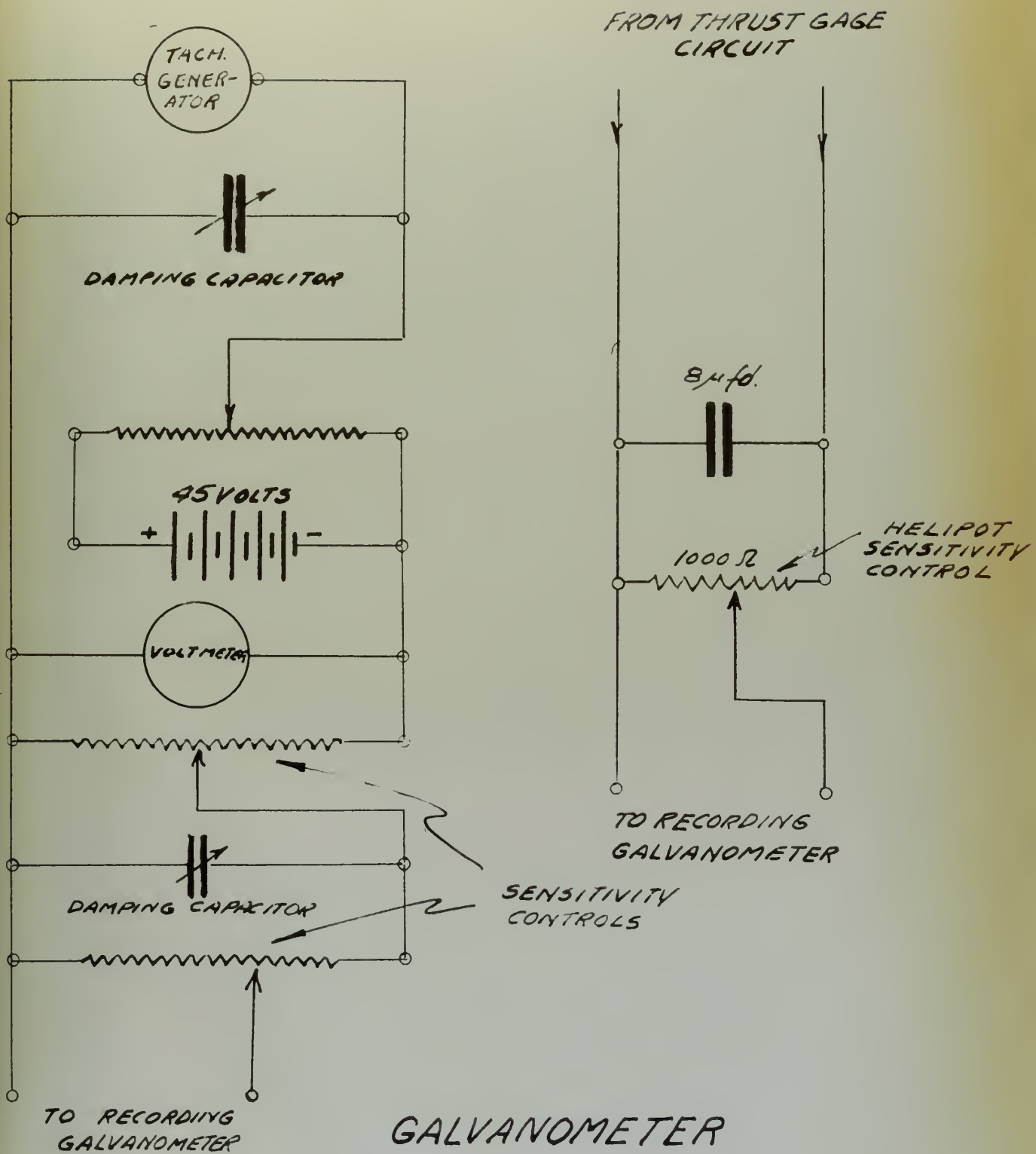

GALVANOMETER SENSITIVITY CONTROL

FIG. 24